Feng, X., Chen, Z. Q., Benton, M. J., Wu, S., Bottjer, D. J., & Thompson, J. R. (2017). A diverse trackway-dominated marine ichnoassemblage from the Lower Triassic in the northern Paleotethys: Ichnology and implications for biotic recovery. *Palaeogeography, Palaeoclimatology, Palaeoecology*. https://doi.org/10.1016/j.palaeo.2017.11.059

A diverse trackway-dominated marine ichnoassemblage from the lowest Triassic in northern Paleo-Tethys: ichnology and implications for biotic recovery

Xueqian Feng[a], Zhong-Qiang Chen[a, *], Michael J. Benton[b], Siqi Wu[a]
[a]*State Key Laboratory of Biogeology and Environmental Geology, School of Earth Science, China University of Geosciences (Wuhan), Wuhan 430074, China*
[b]*School of Earth Sciences, University of Bristol, Bristol BS8 1RJ, UK*
*Corresponding author (ZQC): e-mail: zhong.qiang.chen@cug.edu.cn

Abstract

Here, we document a diverse ichnoassemblage from the marine interbeds of the Lower Triassic terrestrial succession in the Houzhougongmiao (HZGM) section of Shaanxi Province, western North China. The integrated biostratigraphic data (bivalve, palynology and conchostracan) reveals that the ichnofossil-bearing marine beds are Griesbachian (Induan, Early Triassic) in age. The marine interbeds are interpreted as the result of the earliest Triassic transgression of the Paleo-Tethys Ocean northward to the southern margin of North China Craton. The HZGM ichnoassemblage includes 17 ichnospecies in 16 ichnogenera and is dominated by the shallow-tier *Asteriacites* and *Biformites* produced by ophiuroids, the scratch marks or trackways *Dimorphichnus*, *Diplichnites*, and *Monomorphichnus* produced by arthropods, with a minor constituent of the fish swimming trace *Undichna*. Of these, the hook-shaped imprints *Biformites*, representing the arm moving impressions of ophiuroids, are reported for the first time from the Lower Triassic. These trace-makers are interpreted to have lived in a low energy, semi-restricted, but oxygenated, shallow embayment environment. Although possessing relatively high ichnodiversity, the HZGM ichnoassemblage differs clearly from other coeval diverse ichnocoenoses in the lack of complex burrow forms (i.e. *Thalassinoides*, *Diplocraterion*, or *Rhizocorallium*) and mixed layer, and in having abundant shallow tiers. Accordingly, the resting trace or trackway-dominated ichnoassemblage from the HZGM section may represent an exceptional ichnofauna, an initial recovery of the trace-maker ecosystem after the Permian-Triassic mass extinction. The trace-makers such as arthropods and ophiuroids perhaps were opportunistic organisms that proliferated in marginal marine settings when other biota were still suffering post-extinction biotic depletion and environmental stresses.

Keywords: Induan; shallow tiers; North China; ophiuroids; recovery; opportunistic organisms

1. Introduction

Early Triassic ichnofaunas have been widely reported from many localities around the world, and they have been well tested as a useful tool for assessing the recovery process and pattern of marine trace-maker organisms (Twitchett and Wignall, 1996; Twitchett, 1999, 2006; Twitchett and Barras, 2004; Pruss and Bottjer, 2004; Beatty et al., 2008; Fraiser and Bottjer, 2009; Zonneveld et al., 2010; Knaust, 2010; Chen et al., 2011, 2012, 2015; Mata and Bottjer, 2011; Hoffmann et al., 2011, 2015; Luo and Chen, 2014; Zhao et al., 2015; Shi et al., 2015;

Foster et al., 2015; Luo et al., 2016; Feng et al., 2017). Most works show that ichnofaunas of the Griesbachian-Dienerian (Induan) interval were depauperate, and that trace-makers did not recover worldwide until the Spathian in terms of various ecological and ichnological proxies, such as ichnodiversity, burrow size, complexity, tiering level, and bioturbation level (Twitchett, 1999; Pruss and Bottjer, 2004; Fraiser and Bottjer, 2009; Chen et al., 2011; Mata and Bottjer, 2011; Zhao et al., 2015; Luo et al., 2016). In particular, the Griesbachian (early Induan) was a tough time for ichnotaxa, which usually appear at very low ichnodiversity, small burrow size, and shallow tiering level, and are dominated by small, simple/unbranching, low-tier burrows or traces (Twitchett and Barras, 2004; Fraiser and Bottjer, 2009; Chen et al., 2011; Mata and Bottjer, 2011; Zhao et al., 2015; Shi et al., 2015; Luo et al., 2016). The Griesbachian substrate is also usually weakly bioturbated and lacks the mixed layer (Hoffmann et al., 2015). Both ichnofaunal and ichnofabric characteristics indicate the lowest recovery level (Stage 1 *sensu* Twitchett, 2006) at that time, although relatively diverse, high-tier ichnoassemblages have also been sporadically reported from higher latitudes. The latter, however, are usually referred to as an anomalous recovery when most other biota still suffered post-extinction biotic depletion and environmental stresses (Wignall et al., 1998; Beatty et al., 2008; Knaust, 2010; Zonneveld et al., 2010; Hofmann et al., 2011).

Here, we document a newly found, relatively diverse marine trackway-dominated ichnoassemblage from marine interbeds in the lowest Triassic terrestrial successions of the Weihe River areas, Shaanxi Province, North China, which was situated on the southern margin of the North China block during the Permian-Triassic (P-Tr) transition (Fig. 1). In North China, terrestrial clastics characterize the P-Tr transition. The uppermost Permian comprises the lower and middle Sunjiagou Formation, while the Lower Triassic consists of the upper Sunjiagou, Liujiagou and Heshanggou Formations (Chu et al., 2015, 2017; Tu et al., 2016). In addition, terrestrial sedimentation has been strongly influenced by pronounced climatic changes over the P–Tr transition. Mixed yellow, greenish and black siliciclastics with coal measures of the Upper Permian formations are overlain by reddish sandstone and mudstone with paleosol beds of the Lower Triassic (Xu et al., 2004; Yu et al., 2005; Tu et al., 2016). Abundant unusual biosedimentary structures (i.e. microbially induced sedimentary structures, MISS) have been proved to be related to the Permian-Triassic mass extinction (PTME).

The marine interbeds are within the massive Upper Permian to Lower Triassic terrestrial successions, and the newly obtained ichnofossils are also associated with marine bivalves, brachiopods, and ophiuroids (Yin and Lin, 1979; Yang et al., 1983; Liu and He, 2000). The ichnofossil-bearing layers therefore have been considered as indications of embayments occurring in the northern Paleo-Tethys Ocean and southern margin of the North China Craton during the earliest Triassic global transgression (Yin and Lin, 1979; Yang et al., 1983). In North China, no earliest Triassic ichnocoenoses have been reported, although some late Early Triassic ichnofossils have been documented from the terrestrial fluvial and lacustrine facies (i.e. Heshanggou Formation) in the western Henan area, North China (Hu et al., 2009, 2015). The newly found ichnoassemblage therefore provide insights into the survival or recovery of trace-makers in some marginal embayment niches immediately after the PTME.

2. Geological background

2.1. Geological setting

The North China Craton experienced extension during the Late Paleoproterozoic, stabilizing as a platform during the Middle Neoproterozoic (Zhai et al., 2000; Zheng et al., 2013; Liu et al., 2015), receiving marine sediments during the Palaeozoic, having a depositional hiatus from the Middle Ordovician to the Carboniferous, and was uplifted and became terrestrial by the amalgamation of the Qaidam, Tarim and Siberia–Mongolia palaeoplates during the Middle–Late Permian (Wang, 1985). Thus, fluvial and lacustrine facies deposits characterize the Upper Permian and Lower Triassic successions across almost the entire North China block (Xu et al., 2004; Yu et al., 2005; Chu et al., 2015, 2017; Tu et al., 2016). However, the southern margin of the North China block faced the northern Palaeo-Tethys ocean, and thus some embayments occurred occasionally, such as the northern Weihe and southern Qilian areas, due to transgression during the earliest Early Triassic (Yin and Lin, 1979; Yang et al., 1983; Liu and He, 2000; Xu et al., 2017).

In addition, terrestrial sedimentation has been strongly influenced by pronounced climatic changes over the P–Tr transition. The mixed yellow, greenish and black siliciclastics with coal measures of the Upper Permian formations are overlain by reddish sandstone and mudstone with paleosol beds of the Lower Triassic (Xu et al., 2004; Yu et al., 2005; Tu et al., 2016).

2.2. Houzhougongmiao (HZGM) section biostratigraphy

The studied HZGM section (GPS: N34º35.033′, E107º35.833′) is located at Shibaling Village within the town of Xifang, Qishan County, Central Shaanxi Province, Western China (Fig. 1), and records a typical terrestrial-marine siliciclastic succession. The Lower Triassic succession is composed of the upper Sunjiagou, Liujiagou, and Heshanggou formations, which are comparable with the coeval units in most areas of the North China (Liu and He, 2000; Yin and Lin, 1979; Yang et al., 1979; Tu et al., 2016) except for the marine interbeds near the P-Tr boundary (Fig. 2). The Sunjiagou Formation consists of grey thick-bedded sandstone interbedded with greenish thin-bedded siltstone in the lower part; reddish sandstone beds interbedded with greenish mudstone in the middle part; and thin-bedded limestone, siltstone, and lavender thin-bedded mudstone in the upper part (Fig. 2). Limestone and sandstone nodules occur occasionally in thin-bedded siltstone or mudstone. Abundant star-shaped traces of *Asteriacites*, arcuate or hook-shaped imprints of *Biformites*, burrows, and arthropod trackways are preserved in the greenish and lavender thin-bedded mudstone of the upper Sunjiagou Formation (Fig. 2). The overlying Liujiagou Formation is dominated by massive purple and reddish quartz sandstone, with minor amounts of conglomerates, and feldspar sandstone (Zhang et al., 2014; Chu et al., 2015; Tu et al., 2016).

Yin and Lin (1979) reported several marine invertebrate assemblages from the greenish and lavender thin-bedded mudstone of the upper Sunjiagou Formation in the HZGM section, and grey thin-bedded siltstone of the lower Liujiagou Formation in the adjacent Zishiya section. The upper Sunjiagou marine fauna includes bivalves *Eumorphotis multiformis*, *Promyalina putiatinensis*, and *Homomya impressa*, and brachiopods *Lingularia* sp., while the

lower Liujiagou assemblage contains the bivalves *Unionites* sp., *Bakevellia costata*, *Pteria* cf. *murchisoni*, and *Palaeoneilo elliptica*, the brachiopod *Mentzelia* sp., and the ophiuroid *"Ophiolepis*"? *shaanxiensis*. Yin and Lin (1979) proposed that the upper Sunjiagou Formation fauna is Induan (early Early Triassic) in age, while the latter is of an early Olenekian (late Early Triassic) age. In contrast, Cheng et al. (1983) considered that these two marine invertebrate faunas documented by Yin and Lin (1979) both occur in the Liujiagou Formation. These authors have also established the palynological *Lundbladispora-Taeniaesporites-Cycadopites* Assemblage of Induan to early Olenekian ages from the marine fossil-bearing strata. In addition, Ouyang and Zhang (1982) also established the *Lundbladispora-Aratrisporites-Taeniaesporites* microfloral assemblage from the upper Sunjiagou Formation in the Denfeng area, northwest Henan Province.

Later, Liu and He (2000) reported abundant conchostracans *Palaeolimnadia* cf. *machaolingensis*, *Palaeolimnadia* cf. *diannanensis*, and *Protomonocarina sinensis* in association with bivalves *Eumorphotis multiformis* and *Bakevellia*, and the *Lundbladispora-Taeniaesporites-Cycadopites* palynological assemblage from the same beds of the upper Sunjiagou Formation in HZGM section. Of these, the *Lundbladispora-Taeniaesporites-Cycadopites* spore assemblage has been widely treated as the first microfloral zone of the Triassic worldwide (Tewari et al., 2015; Yu et al., 2015). Accordingly, all lines of evidence show that the marine fossil-bearing strata of the upper Sunjiagou Formation in the HZGM section is Griesbachian (early Induan) in age, and the marine ichnoassemblage documented here is also of a Griesbachian age.

2.3 Depositional setting

The Sunjiagou Formation, ~500 m thick, consists of grey thick-bedded sandstone interbedded with greenish thin-bedded siltstone in the lower part; reddish sandstone beds interbedded with greenish mudstone in the middle part; and thin-bedded limestone, siltstone together with lavender thin-bedded mudstone in the upper part (Figs. 2, 3). The basal grey thick-bedded sandstones are poorly exposed; the reddish sandstone beds, ~80 m thick, of the middle part yield rare body fossils; trace fossils are also rarely found, but are typically small, simple, horizontal *Planolites* burrows where they do occur. Thin-bedded siltstone and mudstone, as well as limestone and sandstone lenses make up the upper part. The ichnoassemblage examined here is documented from the thin-bedded siltstone interbedded with greenish mudstone horizons of the upper Sunjiagou Formation. The examined succession ~30 m thick, is composed of two small cycles of the siltstone interbedded with mudstone, as well as one thin-bedded fine-grain sandstone at the top of each cycle in the lower part; and thin-bedded greenish and purple siltstone and light green mudstone in the upper part. Slight ripple marks occasionally occur on the upper surface of the siltstone of the small cycle of the lower part, and the thin-bedded sandstone at the top of the small cycle yields low-angle cross-bedding. Trace fossils are common in the two small cycles of the lower part, while bivalve, conchostracan and gastropod fossils occur in the upper part (Fig. 3H–G). Horizontal bedding is commonly present in siltstone beds throughout the examined succession. Thus, both lithofacies and paleoecology suggest that the ichnofossil-rich succession was likely deposited in a low-energy, semi-restricted, but oxygenated, shallow embayment.

Nevertheless, most interior areas of the North China Craton experienced fewer impacts of the Early Triassic transgression that originated from the Paleo-Tethys Ocean. The upper Sunjiagou Formation therefore is dominated by reddish mudstone, siltstone and yellow thin- to medium-bedded fresh-water limestone, and is usually interpreted to represent a distal fluvial to lake delta setting (Chu et al., 2015, 2017; Tu et al., 2016).

3. Material and methods

Trace fossil taxonomic identification is based on field observations and descriptions of specimens collected from outcrop. Measurements of burrow diameters were undertaken on bedding planes and in vertical exposures following Pruss and Bottjer (2004). Most burrow diameters were measured at the part of the burrow that was most representative of the average width. The maximum length of *Asteriacites* arms was measured from the central point to the tip, and their widest width was measured at the base; the diameters of the central disc-shaped area were measured from the attachment to the arms. The diameters of *Biformites* were measured at the bolder end. Bedding plane bioturbation indices (BPBI) was employed to determine the approximate percentage of bedding planes covered by burrows (Miller and Smail, 1997). In addition, we also considered the "*Ophiolepis*"? *shaanxiensis* specimens described by Yang et al. (1979), as the potential trace maker of *Asteriacites* and *Biformites* from the HZGM section.

4. Results

The marine ichnoassemblage is characterized by star-shaped traces of *Asteriacites*, arcuate or hook-shaped imprints of *Biformites* and various trackways. *Asteriacites* results from the resting activity of sea stars (Asteroidea) and brittle stars (Ophiuroidea), while *Biformites* is interpreted to be the imprints of arms of walking ophiuroids or asterozoans. Traces of brittlestars such as *Asteriacites* and *Biformites* are relatively uncommon in fossil record, and few specimens have been previously reported (Aronson, 1989, 1992; Bell, 2004; Martínez et al., 2009). In contrast, brittlestars are very abundant in the HZGM ichnoassemblage. Interestingly, ophiuroid fossils are also very common in the marine interbeds of the Sunjiahou Formation in the Shaanxi areas. For instance, Yang et al. (1979) described a new species of Ophiuroidea, "*Ophiolepis*"? *shaanxiensis*, from the lowest Triassic of the adjacent Zishiya section of the Linyou area, ~20 km north of the HZGM section.

4.1 Ichnodiversity

The Griesbachian ichnoassemblage includes 17 ichnospecies in 16 ichnogenera (Figs. 4–8): *Arenicolites* isp., *Asteriacites lumbricalis*, *Biformites zhadaensis*, *Dendrotichnium* isp., *Didymaulichnus lyelli*, *Dimorphichnus* isp., *Diplichnites* isp., *Kouphichnium* isp., *Laevicyclus mongraensis*, *Monomorphichnus* isp., *Phycodes* isp., *Planolites montanus*, *Planolites* isp., *Protovirgularia* isp., *Ptychoplasma* isp., *Treptichnus pedum*, and *Undichna* isp. Of these, *Asteriacites lumbricalis*, *Biformites insolitus*, and various trackways (*Dimorphichnus* isp., *Diplichnites* isp., and *Monomorphichnus* isp.) dominate the ichnocoenoses (Fig. 9).

4.2 Ichnology of Asteriacites and *Biformites*

Knaust and Neumann (2016) proposed a new classification scheme for the ichnogenus *Asteriacites*. Three ichnospecies: *A*. *lumbricalis* von Schlotheim, 1820, *A*. *stelliformis* (Miller and Dyer, 1878) Osgood, 1970, and *A*. *quinquefolius* (Quenstedt, 1876) Seilacher, 1953 were established based on decreasing length/width ratio of their arm imprints. Of these, *A*. *lumbricalis* is the type ichnospecies. Several HZGM specimens are assignable to *A*. *lumbricalis*, diagnosed by the central disc-shaped area of pentagonal outline with five large length/width ratio arms originating from its corners. The arms of *A*. *lumbricalis* documented from HZGM are 10–20 mm long, 2 mm wide, and the central disc measures ca. 5 mm (Figs. 4, 10B). The length/width ratio of the arms is 5–10 (Figs. 4, 10A). *A*. *lumbricalis* is characterised by a pentagonal central disc and slender arms with great length/width ratio (Fig. 4). In addition, *A*. *lumbricalis* is exclusively produced by ophiuroids, as indicated by the imprint of a distinct central disc, a morphological character lacking in asteroids (Mikuláš, 1990; Mángano et al., 1999; Wilson and Rigby, 2000; Bell, 2004; Schatz et al., 2013; Baucon and De Carvalho, 2016; Knaust and Neumann 2016).

The ichnogenus *Biformites* is interpreted as produced by ophiuroids and asteroids through locomotion on the sediment surface. Narrow, bedding-parallel, hook-shaped or sinuous imprints characterize this ichnogenus. Knaust and Neumann (2016) proposed a revised scheme of *Biformites*, which includes *B*. *insolitus* Linck, 1949 and *B*. *zhadaensis* (Yang and Song, 1985). Yang and Song (1985) erected a new ichnogenus and ichnospecies, *Zhadaichnus zhadaensis*, from the Triassic turbidites of Tibet. Later, Bell (2004) described similar material as *Ophioichnus aysenensis* Bell, 2004, which is identical with *Z*. *zhadaensis* in its overall morphology. Knaust (2012) therefore regarded *O*. *aysenensis* Bell, 2004 as a junior synonym of *Z*. *zhadaensis*. More recently, Knaust and Neumann (2016) re-assigned *Z*. *zhadaensis* to *Biformites* based on the pronounced imprints of their central discs. This unique ichnospecies is interpreted as a resting trace of ophiuroids here.

The HZGM specimens are assignable to *Biformites zhadaensis* by their delicate, ideally bisymmetrically arranged, transverse (elongate, or polygonal) protuberances of the imprints of arms of walking ophiuroids (Bell, 2004; Schlirf, 2012; Knaust and Neumann, 2016). The HZGM *B*. *zhadaensis* (Fig. 5) possesses burrows 1–3 mm in diameter, with average diameter of 1.8 mm (Fig. 10C).

4.3 Other traces and trackways

In the HZGM ichnoassemblage, burrows are relatively rare (Fig. 9). Vertical burrows such as *Arenicolites* and *Laevicyclus* occur only in sandstone beds (Figs. 2, 6). Burrow sizes of all trace forms are rather small, < 5 mm in diameter. Occasionally, they are preserved as convex epireliefs, together with trackways. Ethologically, the HZGM burrow ichnotaxa are categorized into three types: domichnia (*Arenicolites* and *Laevicyclus*), repichnia (*Didymaulichnus*, *Protovirgularia* and *Ptychoplasma*), and fodinichnia (*Planolites*, *Treptichnus*, and *Phycodes*) (Fig. 6). Overall, burrows are dominated by rather simple, horizontal forms, and the HZGM ichnocoenoses lack relatively complex burrow networks (i.e.

Thalassinoides and *Rhizocorallium*) or deeper tiers such as *Diplocraterion*.

Trackways are very abundant and often associated with *Asteriacites* and *Biformites*. Scratch marks such as *Dimorphichnus* and *Monomorphichnus* are conspicuous among the HZGM ichnotaxa. *Dimorphichnus* comprises asymmetrical trackways involving two types of imprints: elongated scratches or raker marks and blunt imprints referred to as pusher marks (Seilacher, 2007; Hofmann et al., 2012). *Dimorphichnus* exhibits numerous repetitive and overlapping sets of scratch-like, sinusoidal, curvilinear or straight rakes opposing sets of blunt pushers, which are typically lacking in *Monomorphichnus*. Imprints vary from 3–10 mm long but are relatively uniform in size within the row. Imprint pace is 7–11 mm and relatively uniform within one series. The ridges of *Monomorphichnus* are equidistant and 15–30 mm long. Spacing between ridges is about 2 mm. Ridges are up to 1 mm wide (Fig. 7). In case of partial preservation, it is not easy to distinguish the two ichnogenera.

Both *Dimorphichnus* and *Monomorphichnus* were originally attributed to the grazing activity of trilobites (Crimes, 1970; Mángano et al., 1996, 2005; Hofmann et al., 2012), and they are unusual in the Early Triassic ichnofossil record (Fig. 7). Given that all trilobites became extinct in the PTME, arthropods such as limulids are considered as the potential trace makers of these two scratch-mark ichnotaxa (Zonneveld et al., 2010; Diedrich, 2011; Hofmann et al., 2012).

Moreover, both *Kouphichnium* and *Diplichnites* are also distinct in the HZGM ichnoassemblage. These two ichnotaxa have been widely reported from strata older or younger than the Early Triassic. Their Induan records are rather sporadic (Briggs et al., 2010). Several rows of *Kouphichnium* tracks have also been reported from the Olenekian Heshanggou Formation of North China (Chu et al., 2017). The external width of *Diplichnites* trackway is 30 mm and the minimum internal width about 10 mm (Fig. 8E–H).

The fish swimming trace *Undichna* is also rather pronounced in HZGM, and it contains a set of sinusoidal drag marks with a common wave length and alignment. Individual drag marks may be continuous, or the troughs/crests may be preferentially absent or preferentially present. There may be up to five sinusoidal elements in a set. Waves occur as non-parallel pairs that are intertwined. The traces are preserved as impressions on the bedding surface of the siltstone (Wisshak et al., 2004). The wave-shaped trace is 25 mm wide and extends over 15 cm across the slab. All waves are ~40 mm in wavelength, and their amplitudes decrease outward from 20 mm to 12 mm. Both the wavelength and amplitude are constant (Fig. 7D). The median ridge is laterally slightly displaced, and may crosscut the lateral ridges. The inner lateral ridges occasionally crosscut the outer lateral pair of ridges. Individual ridges are up to 1 mm wide. *Undichna* traces are all preserved as hypichnial ridges from the same bed. Interestingly, *Undichna* has rarely been reported from the Lower Triassic successions worldwide, although the first record of this ichnogenus was found in the Spathian Jialingjiang Formation, Sichuan Province, Southwest China (Lu et al., 2012).

5. Discussion

5.1 Taphonomy and ecology of Asteriacites *and* Biformites*, and their possible trace-makers*

Asteriacites is preserved as convex hyporeliefs on sandstone beds in the HZGM section,

and is characterized by a pentagonal central disc and slender arms with great length/width ratio (Fig. 4). These characteristics agree well with *A. lumbricalis* (Knaust and Neumann, 2016), which is usually believed to have been produced by ophiuroids because of the imprint of a distinct central disc, a morphological character lacking in asteroids. *A. lumbricalis* reflects a burrowing or resting behaviour where both the disc and the arms are buried together. The ophiuroid buries itself in sediment by swinging movements of the central disc, while leaving its arms spread and at rest. The ends of some ophiuroid arms not buried in the substrate may move laterally so as to produce repetitive traces with ramifying arms (Fig. 11A).

Biformites zhadaensis is very abundant on thin-bedded siltstone bedding planes, especially from neighbouring horizons below and above the *A. lumbricalis*-bearing sandstone beds. Few specimens occur on the same sandstone beds with *A. lumbricalis*. Most imprints are preserved as convex epireliefs, but concave epireliefs also occur occasionally (Fig. 5). The combination of a cluster of arcuate or hook-shaped imprints, slightly tapering terminations, together with bisymmetrically arranged, transverse protuberances distinguishes *B. zhadaensis* from most burrow-form traces and makes it similar to the casts of ophiuroid arms. Undoubtedly, *B. zhadaensis* with hook-like structures most likely records the slender, sinuous arm impressions of ophiuroid echinoderms when moving on the substrate (Fig. 11B). Series of hook-shaped imprints can be identified from the examined beds, while isolated individuals are also occasionally present. The imprints are always parallel to the bedding planes, with an extremely shallow penetration. These Sunjiagou Formation specimens are unique to the studied area, and have never been reported from coeval or younger Early Triassic successions elsewhere in the world.

The most likely trace-makers of both *A. lumbricalis* and *B. zhadaensis* are ophiuroids. Ophiuroid body and trace fossils are relatively common in lowest Triassic successions worldwide (Yang et al., 1979; Feng, 1985; Chen et al., 2004; Twitchett et al., 2005; Chen and McNamara, 2006; Seilacher, 2007; Jaselli, 2014; Baucon and De Carvalho, 2016). The Lower Triassic ophiuroid fossils are preserved in a great variety of lithologies, varying from greenish shale to calcareous mudstone, limestone, and dolomitic limestone, indicating a wide range of depositional settings from nearshore, siliciclastic shallow seas, to open platform, ramp to deep sea (Chen and McNamara 2006). Thus, ophiuroids represent an outstanding example of a group that profited from the re-organization of ecosystems after the PTME ecological crisis (Chen and McNamara, 2006). The presence of abundant *A. lumbricalis* and *B. zhadaensis* traces reinforces the proliferation of ophiuroids after the PTME.

In addition, like these extant forms, the Early Triassic ophiuroids likely started to disarticulate within a few hours after their death (Twitchett et al., 2005). This is why so many isolated arm imprints, rather than complete ophiuroid imprints, are present in the HZGM collections. As the above facies analysis inidcates, these ophiuroids probably lived in a low-energy, semi-restricted, but oxygenated, shallow embayment setting.

In HZGM, both *A. lumbricalis* and *B. zhadaensis* show very shallow penetration into the sediment, indicating that the trace-producing ophiuroids were relatively shallow burrowers. Their burrows (i.e. *Asteriacites* and *Biformites*) therefore are easily destroyed by deeper burrowers and strong bioturbation.

In general, the aftermath of the PTME is characterised by very shallow tiers and low

levels of bioturbation (Bottjer and Ausich 1986; Twitchett and Barras 2004). According to Chen and McNamara (2006), ophiuroids profited greatly from the end-Permian crisis by undergoing a significant diversification in the post-extinction oceans, following Erwin's model of a "logistic increase in diversity beginning immediately after the end of the mass extinction" (Erwin 2000, 2001). The ophiuroid recovery occurred within 1–2 million years, which is much shorter than that of other clades, such as gastropods and reef builders after the PTME. The post-extinction ophiuroids radiated in the Olenekian (Chen and McNamara, 2006).

5.2 Comparisons with coeval ichnoassemblages elsewhere in the world

Lower Triassic ichnoassemblages have been widely reported from around the world (Twitchett and Wignall, 1996; Wignall et al., 1998; Twitchett, 1999; Pruss and Bottjer, 2004; Beatty et al., 2008; Fraiser and Bottjer, 2009; Hu et al., 2009, 2015; Knaust, 2010; Zonneveld et al., 2010; Hofmann et al., 2011, 2015; Mata and Bottjer, 2011; Chen et al., 2011, 2012, 2015; Lovelace and Lovelace, 2012; Foster et al., 2015; Shi et al., 2015; Zhao et al., 2015; Baucon and De Carvalho, 2016; Bordy and Krummeck, 2016; Luo et al., 2016; Uchman et al., 2016; Feng et al., 2017) (Fig. 12). In most cases, ichnoassemblages did not diversify until the Olenekian, especially in the Spathian, even if in different settings (Fig. 12). Induan trace fossils are unusual, and mainly represented by simple, horizontal *Planolites* burrows (Figs. 12, 13A). Spathian ichnoassemblages are always more than ten ichnospecies, representing a relatively high ichnodiversity (Fig. 12).

However, in rare cases, the Griesbachian (or Induan) ichnofauna also diversified, and almost reached the same ichnotaxic level or even more than those commonly in the Smithian and Spathian (Fig. 12). These anomalously diverse ichnocoenoses are reported from the Svalbard, western Spitsbergen (Wignall et al., 1998), from Alberta and British Columbia, western Canada (Beatty et al., 2008; Zonneveld et al., 2010), from the Persian Gulf, Iran (Knaust, 2010), and from the Dolomites, Italy (Hofmann et al., 2011). Our diverse Induan ichnoassemblage is from the western part of North China (Fig. 12).

Twelve Dienerian ichnotaxa were recognized from shoreface sandstone beds of the Vardebukta Formation from Boreal sections of Spitsbergen, among which are included the complex burrow forms *Thalassinoides* and *Rhizocorallium*, while both *Zoophycus* and *Chondrites* are excluded. Thus, the post-extinction ichnological recovery in Spitsbergen was more rapid than in the Palaeo-Tethys region. In addition, the same successions also yield an appreciable diversity of fauna, including bryozoans, calcareous algae, and deep infaunal bivalves, suggesting that the marine ecosystem recovery began first in higher palaeolatitudes (Wignall et al., 1998).

Diverse and abundant Griesbachian marine invertebrate ichnoassemblages (> 30 ichnotaxa) are described from the Montney Formation of northwestern Alberta and northeastern British Columbia of western Canada. The ichnocoenoses are dominated by arthropod-constructed forms (*Thalassinoides* and *Rhizocorallium*), which commonly occur in intensely bioturbated (ii 5) sandstone beds. These 'anomalously diverse' ichnoassemblages are believed to have been strongly controlled by environmental conditions which occurred in a lower shoreface to offshore transition 'habitable zone' settings (Beatty et al., 2008;

Zonneveld et al., 2010).

After a detailed study of carbonate well cores of the Khuff Formation from the Persian Gulf, Iran, Knaust (2010) described 13 ichnogenera from the Induan. Of these, *Diplocraterion* occurred ~55 cm above the PTB and was the first Triassic trace fossil in the studied sections. *Diplocraterion* has a limb diameter of 1 mm, spreiten width of 5–7 mm, spreiten length of 15 mm, and a penetration depth down to 4 cm. Such a diverse ichnoassemblage from a low-latitude carbonate platform from the Persian Gulf suggests that refuges are not restricted to high latitudes, but also occur in equatorial settings, and that biotic recovery took no longer in equatorial regions than in northerly palaeolatitudes (Wignall et al., 1998; Twitchett and Barras, 2004; Twitchett et al., 2004; Beatty et al., 2008; Zonneveld et al., 2010; Knaust, 2010).

Ten ichnotaxa have also been recognized from mixed siliclastic-carbonate shelf sediments of the late Griesbachian Werfen Formation of the Dolomites, northern Italy. The large, complex burrow forms *Thalassinoides*, *Spongeliomorpha* and *Rhizocorallium* are distinct in the Dolomite ichnoassemblage. These high-tier ichnotaxa indicate that a significant global recovery of benthic ecosystems may have occurred soon after the PTME, and that the early recovery of trace makers was not latitudinally restricted (Hofmann et al., 2011).

To sum up, known diverse Induan ichnocoenoses show that: (1) high ichnodiversity may occur at both high and low latitudes; (2) deep-tier, complex burrow forms such as *Thalassinoides*, *Diplocraterion*, and *Rhizocorallium* may also occur in the Griesbachian (Figs. 12, 13C); (3) the bioturbation level, indicated by ichnofabric indices (ii) and bedding plane bioturbation indices (BPBI), of the ichnofossil-bearing strata can also occasionally reach a high level in the Induan, although they mostly remain at low level.

When compared with coeval diverse ichnocoenoses elsewhere in the world, we found that the HZGM ichnoassemblage lacks complex burrow forms (i.e. *Thalassinoides*, *Diplocraterion*, or *Rhizocorallium*), and is dominated by the ophiuroid traces *Asteriacites* and *Biformites*, and the arthropod trackways *Dimorphichnus*, *Monomorphichnus*, and *Diplichnites* (Figs. 9, 13B). The fish swimming trace *Undichna* is also rather pronounced.

5.3 Ichnological evidence indicating biotic recovery after the PTME

In HZGM, the vertical burrows *Arenicolites* and *Laevicyclus* are very rare, most ichnofossils are shallow-tier burrow systems such as *Treptichnus*, *Asteriacites* and *Biformites*, which were likely produced by ophiuroids (Baucon and De Carvalho, 2016; Knaust and Neumann 2016) (Figs. 9, 11).

Like other coeval diverse ichnocoenoses that usually inhabit open, oxygenated, shallow marine settings, the HZGM ichnotaxa also lived in an oxygenated, shallow embayment, although the substrates may indicate semi-restricted and low-energy, calm environments.

The preference for shallow marine settings of the diverse Griesbachian (or Dienerian) ichnocoenoses suggests that environmental setting is an important factor shaping trace-maker recovery during the Induan. Conversely, shallow marine settings do not ensure the proliferation of the Induan ichnocoenoses, implying that environmental settings may not be the only factor affecting the post-extinction recovery of the trace-makers, and that other elements such as oxygen level and taphonomic conditions may have been equally important.

In addition, most localities which only contain *Planolites* or much lower ichnodiversity ichnoassemblages during the Induan, but saw the peak of the ichnodiversity richness during the Olenekian, especially in the Spathian, indicate that time is also a significant element for the recovery of trace-makers (Fig. 12).

When compared with coeval, highly diversified ichnocoenoses, the HZGM ichnoassemblage shows some striking discrepancies: lack of the complex burrow forms *Thalassinoides*, *Diplocraterion*, or *Rhizocorallium*; predominance of shallow-tier *Asteriacites* and *Biformites* and arthropod trackways; lack of mixed layers; and having a low bioturbation level. Accordingly, the HZGM trace forms may represent an exceptional ichnoassemblage, which is distinguished from most burrow-form ichnocoenoses recorded elsewhere in the world (Fig 13B). All lines of evidence indicate that the ecosystem had still not fully recovered. Common trace-makers such as arthropods and ophiuroids perhaps were opportunistic organisms when other biota still suffered post-extinction biotic depletion and environmental stresses during the earliest Triassic.

6. Conclusions

A diverse ichnoassemblage is documented from the marine interbeds of the Induan (Early Triassic) terrestrial succession of the HZGM section of Shaanxi, in western North China. These marine interbeds are interpreted as the result of the transgression of the Palaeo-Tethys Ocean northward to the southern margin of the North China Craton during the earliest Triassic. The HZGM ichnoassemblage includes 17 ichnospecies in 16 ichnogenera and is characterized by the shallow-tier *Asteriacites* and *Biformites* produced by ophiuroids, scratch marks or trackways *Dimorphichnus*, *Diplichnites*, and *Monomorphichnus* produced by arthropods, together with the fish swimming trace *Undichna*. The hook-shaped imprints *Biformites*, representing the arm moving impressions of ophiuroids, are reported for the first time from the Lower Triassic. The HZGM ichnoassemblage is interpreted to inhabit a low-energy, semi-restricted but oxygenated, shallow embayment setting. When compared with coeval diverse ichnocoenoses, the HZGM ichnoassemblage lacks complex burrows (i.e. *Thalassinoides*, *Diplocraterion*, or *Rhizocorallium*) and is dominated by shallow tiers and arthropod trackways, together with the fish swimming trace *Undichna*, and thus may represent an exceptional ichnoassemblage indicating that the tracemaker-dominated ecosystem was still not fully recovered during the Griesbachian (Early Triassic). Abundant trace-makers (i.e. arthropods and ophiuroids) perhaps were opportunists and proliferated in the marginal marine setting when other biota still suffered post-extinction biotic depletion and environmental stresses during the earliest Triassic.

Acknowledgements

We thank Yaling Xu, Chengyi Tu, Zeming Zheng, Guojing Zhang, and Hongfei Chen for their assistance in the field. This study was supported by the 111 Program of China, Ministry of Education of China (B08030), two NSFC research grants (41272023, 41572091), one research grant from the State Key Laboratory of Geological Processes and Mineral Resources (GPMR201302), China University of Geosciences.

References

Aronson, R.B., 1989. A community-level test of the Mesozoic Marine Revolution theory. Paleobiology 15, 20–25.

Aronson, R.B., 1992. Biology of a scale-independent predator-prey interaction. Marine Ecol. Progr. Ser. 89, 1–13.

Baucon, A., De Carvalho, C.N., 2016. Stars of the aftermath: *Asteriacites* beds from the Lower Triassic of the Carnic Alps (Werfen Formation, Sauris di Sopra), Italy. Palaios 31, 161–176.

Beatty, T.W., Zonneveld, J.-P., Henderson, C.M., 2008. Anomalously diverse Early Triassic ichnofossil assemblages in northwest Pangea: a case for a shallow-marine habitable zone. Geology 36, 771–774.

Bell, C.M., 2004. Asteroid and ophiuroid trace fossils from the Lower Cretaceous of Chile. Palaeontology 47, 51–66.

Bordy, E.M., Krummeck, W.D., 2016. Enigmatic continental burrows from the Early Triassic transition of the Katberg and Burgersdorp formations in the main Karoo Basin, South Africa. Palaios 31, 389–403.

Bottjer, D.J., Ausich, W.I., 1986. Phanerozoic development of tiering in soft substrata suspension-feeding communities. Paleobiology 12, 400–420.

Briggs, D.E.G., Miller, M.F., Isbell, J.L., Sidor, C.A., 2010. Permo-Triassic arthropod trace fossils from the Beardmore Glacier area, central Transantarctic Mountains, Antarctica. Antarctic Sci. 22, 185–192.

Buatois, L.A., Almond, J., Germs, G.J.B., 2013. Environmental tolerance and range offset of *Treptichnus pedum*: Implications for the recognition of the Ediacaran-Cambrian boundary. Geology 41, 519–522.

Chen, Z.Q., McNamara, K.J., 2006. End-Permian extinction and subsequent recovery of the Ophiuroidea (Echinodermata). Palaeogeogr. Palaeoclimatol. Palaeoecol. 236, 321–344.

Chen, Z.Q., Shi, G.R., Kaiho, K., 2004. New ophiuroids from the Permian–Triassic boundary beds of South China. Palaeontology 47, 1301–1312.

Chen, Z.Q., Tong, J.N., Fraiser, M.L., 2011. Trace fossil evidence for restoration of marine ecosystems following the end-Permian mass extinction in the Lower Yangtze region, South China. Palaeogeogr. Palaeoclimatol. Palaeoecol. 299, 449–474.

Chen, Z.Q., Fraiser, M.L., Bolton, C., 2012. Early Triassic trace fossils from Gondwana interior sea: Implication for ecosystem recovery following the end-Permian mass extinction in south high-latitude region. Gondwana Res. 22, 238–255.

Chen, Z.Q., Yang, H., Luo, M., Benton, M.J., Kaiho, K., Zhao, L.S., Huang, Y.G., Zhang, K.X., Fang, Y.H., Jiang, H.S., Qiu, H., Li, Y., Tu, C.Y., Shi, L., Zhang, L., Feng, X.Q., Chen, L.,2015. Complete biotic and sedimentary records of the Permian–Triassic transition from Meishan section, South China: Ecologically assessing mass extinction and its aftermath. Earth-Sci. Rev. 149, 67–107.

Cheng, Z.W., Qu, L.F., Hou, J.P., Li, P.X., 1983. The stratigraphic question of *Eumorphotis*-bearing 'Shiqianfeng' Formation in Qishan, Shaanxi Province. J. Stratigr. 7, 161–168.

Chu, D.L., Tong, J.N., Song, H.J., Benton, M.J., Bottjer, D.J., Song, H.Y., Tian, L., 2015. Early Triassic wrinkle structures on land: stressed environments and oases for life. Sci. Report. 5, e10109. http://dx.doi.org/10.1038/srep10109.

Chu, D.L., Tong, J.N., Bottjer, D.J., Song, H.J., Song, H.Y., Benton, M.J., Tian, L., Guo, W.W., 2017. Microbial mats in the terrestrial Lower Triassic of North China and implications for the Permian–Triassic mass extinction. Palaeogeogr. Palaeoclimatol. Palaeoecol. 474, 214–231.

Crimes, T. P., 1970. Trilobite tracks and other trace fossils from the upper Cambrian of North Wales. Geol. J. 7, 47–68.

Diedrich, C., 2011. Middle Triassic horseshoe crab reproduction areas on intertidal flats of Europe with evidence of predation by archosaurs. Biol. J. Linn. Soc. 103, 76–105.

Droser, M.L., Bottjer, D.J., 1986. A semiquantitative field classification of ichnofabric. J. Sediment. Petrol. 56, 558–559.

Erwin, D.H., 2000. Life's downs and ups. Nature 404, 129–130.

Erwin, D.H., 2001. Lessons from the past: biotic recoveries from mass extinctions. The end and the beginning: recoveries from mass extinctions. Proc. Natl. Acad. Sci. U.S.A. 98, 5399–5403.

Feng, R.L., 1985. New discovery of fossil ophiuroids from Guizhou and southern Sichuan, China. Ac. Palaeontol. Sin. 24,337–343.

Feng, X.Q., Chen, Z.Q., Woods, A.D., Fang, Y.H., 2017. A Smithian (Early Triassic) ichnoassemblage from Lichuan, Hubei Province, South China: implications for biotic recovery after the latest Permian mass extinction. Palaeogeogr. Palaeoclimatol. Palaeoecol (in press).

Foster, W.J., Danise, S., Sedlacek, A., Price, G.D., Hips, K., Twitchett, R.J., 2015. Environmental controls on the post-Permian recovery of benthic, tropical marine ecosystems in western Palaeotethys (Aggtelek Karst, Hungary). Palaeogeogr. Palaeoclimatol. Palaeoecol. 192, 374–394.

Fraiser, M.L., Bottjer, D.J., 2009. Opportunistic behavior of invertebrate marine tracemakers during the Early Triassic aftermath of the end-Permian mass extinction. Aust. J. Earth Sci. 56, 841–857.

Häntzschel, W., 1975. Trace fossils and problematica. In: Teichert, C. (Ed.), Treatise of Invertebrate Paleontology (2nd Edition), Part W, Miscellanea, Supp 1. University of Kansas and Geological Society of America, Lawrence, Kansas, 269 pp.

Hofmann, R., Goudemand, N., Wasmer, M., Bucher, H., Hautmann, M., 2011. New trace fossil evidence for an early recovery signal in the aftermath of the end-Permian mass extinction. Palaeogeogr. Palaeoclimatol. Palaeoecol. 310, 216–226.

Hofmann, R., Mangano, M.G., Elicki, O., Shinaq, R., 2012. Paleoecologic and biostratigraphic significance of trace fossils from shallow- to marginal-marine environments from the Middle Cambrian (Stage 5) of Jordan. J. Paleontol. 86, 931–955.

Hofmann, R., Buatois, L.A., MacNaughton, R.B., Mangano, M.G., 2015. Loss of the sedimentary mixed layer as a result of the end-Permian extinction. Palaeogeogr. Palaeoclimatol. Palaeoecol. 428, 1–11.

Hu, B., Yang, W.T., Song, H.B., Wang, M., Zhong, M.Y., 2009. Trace Fossils and Ichnofabrics in the Heshanggou Formation of lacustrine deposits, Jiyuan area, Henan

Province. Acta Sedimentol. Sin. 27, 573–582.
Hu, B., Lu, X.H., Song, H.B., 2015. Lower Triassic ichnofossils and sedimentary environments in the Dengfeng area, western Henan Province. J. Stratigr. 39, 454–465.
Jaselli, L., 2014. The first occurrence of ophiuroids (Ophiuroidea, Echinodermata) in the Early Triassic of Lombardy (Northern Italy). Atti della Società Toscana di Scienze Naturali, Memorie, Serie A. 121, 47–54.
Knaust, D., 2010. The end-Permian mass extinction and its aftermath on an equatorial carbonate platform: insights from ichnology. Terra Nova 22, 195–202.
Knaust, D., 2012. Trace-fossil systematics. In: Knaust, D., Bromley, R.G. (Eds.), Trace Fossils as Indicators of Sedimentary Environments. Developments in Sedimentology Vol. 64, pp. 79–101.
Knaust, D., Warchol, M., Kane, I.A., 2014. Ichnodiversity and ichnoabundance: Revealing depositional trends in a confined turbidite system. Sedimentology 61, 2218–2267.
Knaust, D., Neumann, C., 2016. *Asteriacites* von Schlotheim, 1820 – the oldest valid ichnogenus name and other asterozoan-produced trace fossils. Earth-Sci. Rev. 157, 111–120.
Lai, X.L., Yin, H.F., Yang, F.Q., 1995. Reconstruction of the Qinling Triassic Paleo- ocean. J. Earth Sci. 20, 648–656.
Linck, O., 1949. Lebens-Spuren aus dem Schilfsandstein (Mittl. Keuper, km 2) NWWürttembergs und ihre Bedeutung für die Bildungsgeschichte der Stufe. Jahreshefte des Vereins für vaterländische Naturkunde in Württemberg 97–101, 1–100.
Liu, S.W., He, Z.J., 2000. Marine conchostracans from the 'Sunjiagou Formation' of Qishan, Shaanxi. Acta Palaeontol. Sin. 39, 230–236.
Liu, Y.Q., Kuang, H.W., Peng, N., Xu, H., Zhang, P., Wang, N.S., An, W., 2015. Mesozoic basins and associated palaeogeographic evolution in North China. J. Palaeogeogr. 4, 189–202.
Lovelace, D.M., Lovelace, S.D., 2012. Paleoenvironments and paleoecology of a Lower Triassic invertebrate and vertebrate ichnoassemblage from the Red Peak Formation Chugwater Group), Central Wyoming. Palaios 27, 636–657.
Lu, T.Q., Wang, Z.L., Yang, X.Y., Zhang, X.L., 2012. First record of Lower Triassic *Undichna* spp. fish swimming traces from Emei, Sichuan Province, China. Chin. Sci. Bull. 57, 1320–1324.
Luo, M., George, A.D., Chen, Z.Q., 2016. Sedimentology and ichnology of two Lower Triassic sections in South China: Implications for the biotic recovery following the end-Permian mass extinction. Glob. Planet. Chang. 144, 198–212.
Mángano, M.G., Buatois, L.A., Acenolaza, G. F., 1996. Trace fossils and sedimentary facies from a late Cambrian–Early Ordovician tide-dominated shelf (Santa Rosita Formation, northwest Argentina): Implications for ichnofacies models of shallow marine successions. Ichnos 5, 53–88.
Mángano, M.G., Buatois, L.A., West, R.R., Maples, C.G., 1999. The origin and paleoecologic significance of the trace fossil *Asteriacites* in the Pennsylvanian of Kansas and Missouri. Lethaia 32, 17–30.
Mángano, M.G., Buatois, L.A., Guinea, F. M., 2005. Ichnology of the Alfarcito Member (Santa Rosita Formation) of northwestern Argentina: Animal-substrate interactions in a

lower Paleozoic wave-dominated shallow sea. Ameghiniana 42, 641–668.
Martinez, S., Delrio, C.J., Perez, D., 2009. A brittle star bed from the Miocene of Patagonia, Argentina. Lethaia 43, 1–9.
Mata, S.C., Bottjer, D.J., 2011. Origin of Lower Triassic microbialites in mixed carbonate–siliciclastic successions: ichnology, applied stratigraphy, and the end-Permian mass extinction. Palaeogeogr. Palaeoclimatol. Palaeoecol. 300, 158–178.
Mikuláš, R., 1990. The ophiuroid *Taeniaster* as a tracemaker of *Asteriacites*, Ordovician of Czechoslovakia. Ichnos 1, 133–137.
Miller, S.A., Dyer, C.B., 1878. Contributions to Palaeontology No. 2. Cincinnati, Ohio (Private Publication) (11 pp., 2 pl.).
Miller, M.F., Smail, S.E., 1997. A semiquantitative method for evaluating bioturbation on bedding planes. Palaios 12, 391–396.
Osgood, R.G., 1970. Trace fossils of the Cincinnati area. Palaeontogr. Am. 6, 281–444.
Ouyang, S., Zhang, Z., 1982. Early Triassic palynological assemblage in Dengfeng, northwestern Henan. Acta Palaeontol. Sin. 21, 685–696.
Pruss, S.B., Bottjer, D.J., 2004. Early Triassic fossils of the western United States and their implications for prolonged environmental stress from the end-Permian mass extinction. Palaios 19, 551–564.
Quenstedt, F.A., 1876. Petrefaktenkunde Deutschlands. 4. Die Asteriden und Encriniden nebst Cysti und Blastoideen. Fuess, Leipzig, 742 pp., pls. 90–114.
Rindsberg, A.K., Kopaska-Merkel, D.C., 2005. *Treptichnus* and *Arenicolites* from the Steven C. Minkin Paleozoic footprint Site (Langsettian, Alabama, USA). In: Buta, R.J., Rindsberg, A.K., Kopaska-Merkel, D.C. (Eds.), Pennsylvanian Footprints in the Black Warrior Basin of Alabama, Monograph 1. Alabama Paleontological Society, pp. 121–141.
Schatz, E.R., Mángano, M.G., Aitken, A.E., Buatois, L.A., 2013. Response of benthos to stress factors in Holocene Arctic fjord settings: Maktak, Coronation, and North Pangnirtung Fjords, Baffin Island, Canada. Palaeogeogr. Palaeoclimatol. Palaeoecol. 386, 652–668.
Schlirf, M., 2012. *Heliophycus seilacheri* n. isp. and *Biformites insolitus* Linck, 1949 (trace fossils) from the Late Triassic of the Germanic Basin: Their taxonomy and palaeoecological relevance. Neues Jahrb. Geol. Paläontol. Abh. 263, 185–198.
von Schlotheim, F., 1820. Die Petrefactenkunde aufihrem jetzigen Standpunkte durch die Beschreibung seiner Sammlung versteinerter und fossiler Überreste des Thier- und Pflanzenreichs der Vorwelt. Becker, Gotha, 438 pp., 15 pl.
Seilacher, A., 1953. Studien zur Palichnologie II. Die fossilen Ruhespuren (Cubichnia). Neues Jahrb. Geol. Paläontol. Abh. 98, 87–124.
Seilacher, A., 2007. Trace Fossil Analysis. Springer, Berlin, 226 pp.
Shi, G., Woods, A.D., Yu, M.Y., Wei, H.Y., 2015. Two episodes of evolution of trace fossils during the Early Triassic in the Guiyang area, Guizhou Province, South China. Palaeogeogr. Palaeoclimatol. Palaeoecol. 426, 275–284.
Tewari, R., Ram-Awatar, Pandita, S.K., McLoughlin, S., Agnihotri, D., Pillai, S.S.K., Singh, V., Kumar, K., Bhat, G.D., 2015. The Permian–Triassic palynological transition in the Guryul Ravine section, Kashmir, India: implications for Tethyan-Gondwanan correlations. Earth-Sci. Rev. 149, 53–66.

Tu, C.Y., Chen, Z.Q., Retallack, G.J., Huang, Y.G., Fang, Y.H., 2016. Proliferation of MISS related microbial mats following the end-Permian mass extinction in terrestrial ecosystems: evidence from the Lower Triassic of the Yiyang area, Henan Province, North China. Sediment. Geol. 333, 50–69.

Twitchett, R.J., 1999. Palaeoenvironments and faunal recovery after the end-Permian mass extinction. Palaeogeogr. Palaeoclimatol. Palaeoecol. 154, 27–37.

Twitchett, R.J., 2006. The palaeoclimatology, palaeoecology and palaeoenvironmental analysis of mass extinction events. Palaeogeogr. Palaeoclimatol. Palaeoecol. 232, 190–213.

Twitchett, R.J., Wignall, P.B., 1996. Trace fossils and the aftermath of the Permo-Triassic mass extinction: evidence from Northern Italy. Palaeogeogr. Palaeoclimatol. Palaeoecol. 124, 137–151.

Twitchett, R.J., Barras, C.G., 2004. Trace fossils in the aftermath of mass extinction events. In: McIlroy, D. (Ed.), Application of Ichnology to Palaeoenvironmental and Stratigraphic Analysis. Geol. Soc. London Spec. Publ. 228, 395–415.

Twitchett, R.J., Krystyn, L., Baud, A., Wheeley, J.R., Richoz, S., 2004. Rapid marine recovery after the end-Permian mass extinction event in the absence of marine anoxia. Geology 32, 805– 808.

Twitchett, R.J., Feinberg, J.M., O'Connor, D.D., Alvarez, W., McCollum, L., 2005. Early Triassic ophiuroids: their paleoecology, taphonomy and distribution. Palaios 20, 213–223.

Uchman, A., Mikulas, R., Rindsberg, A.K., 2011. Mollusc trace fossils *Ptychoplasma* Fenton and Fenton, 1937 and *Oravaichnium* Plicka and Uhrova, 1990: their type material and ichnospecies. Geobios 44, 387–397.

Uchman, A., Hanken, N.M., Nielsen, J.K., Grundvag, S.A., Piasecki, S., 2016 Depositional environment, ichnological features and oxygenation of Permian to earliest Triassic marine sediments in central Spitsbergen, Svalbard. Polar Res. 35, 24782. http://dx.doi.org/10.3402/polar.v35.24782.

Wang, H.Z. (Ed.), 1985. Atlas of the Palaeogeography of China. Cartographic Publishing House, Beijing, 281 pp. (in Chinese).

Wignall, P.B., Morante, R., Newton, R., 1998. The Permo–Triassic transition in Spitsbergen: $\delta^{13}C_{org}$ chemostratigraphy, Fe and S geochemistry, facies, fauna and trace fossils: Geol. Mag. 135, 47–62.

Wilson M.A., Rigby, J. K., 2000. *Asteriacites lumbricalis* von Schlotheim 1820: Ophiuroid trace fossils from the lower Triassic Thaynes Formation, central Utah. Ichnos 7, 43–49.

Wisshak, M., Volohonsky, E., Blomeier, D., 2004. Acanthodian fish trace fossils from the Early Devonian of Spitsbergen. Acta Palaeontol. Pol. 49, 629–634.

Xu, H., Zhao, Z., Lu, F., Yang, Y., Tang, Z., Sun, G., Xu, Y., 2004. Tectonic evolution of the Nanhuabei area and analysis about its petroleum potential. Geotectonica et Metallogenia 28, 450–463.

Xu, Y.L., Chen, Z.Q., Feng, X.Q., Wu, S.Q., Tu, C.Y., 2016. Proliferation of MISS-related microbial mats following the end-Permian mass extinction in northern margins of the Paleo-Tethys Ocean: evidence from southern Qilianshan region, western China. Palaeogeogr. Palaeoclimatol. Palaeoecol. 474, 198–213.

Yang, S., Song, Z., 1985. Middle-Upper Triassic trace fossils from Zhada, Ngari, Southwest Xizang (Tibet), and its geologic significance. Xizang (Tibet) Geol. 1, 1–14 (pl. I–IV.).

Yang, Z.Y., Yin, H.F., Lin, H.M., 1979. Marine Triassic faunas from Shihchienfeng Group in the northern Weihe River Basin, Shaanxi Province. Acta Palaeontol. Sin. 18, 465–474.

Yang, Z.Y., Yin, H.F., Xu, G.R., Wu, S.B., 1983. The Triassic of the South Qilian Mountain: Beijing, Geological Publishing House, 259 pp.

Yin, H.F., Lin, H.M., 1979. Marine Triassic faunas and the geologic time from Shihchienfeng Group in the northern Weihe River Basin. J. Stratigr. 3, 233–241.

Yu, H.Z., Lu, F.L., Guo, Q.X., Lu, W.Z., Wu, J.Y., Han, S.H., 2005. Proto sediment basin types and tectonic evolution in the southern edge of North China Plate. Petroleum Geology and Experiment 27, 111–117.

Yu, J.X., Broutin, J., Chen, Z.Q., Shi, X., Li, H., Chu, D.L., Huang, Q.S., 2015. Vegetation changeover across the Permian–Triassic Boundary in Southwest China: Extinction, survival, recovery and paleoclimate: a critical review. Earth-Sci. Rev. 149, 203–224.

Zhai, M. G., Bian, A. G., Zhao, T. P., 2000. The amalgamation of the supercontinent of North China Craton at the end of Neoarchean, and its break up during the Late Paleoproterozoic and Mesoproterozoic. Sci. Chin. D Earth Sci. 43, 219–232.

Zhang, L., Yang, W., Niu, Y., 2014. Characteristic and geological significance of microbially induced sedimentary structures (MISS) in terrestrial P–Tr boundary in western Henan. Acta Palaeontol. Sin. 60, 1051–1060.

Zhao, X., Tong, J., Yao, H., Niu, Z., Luo, M., Huang, Y., Song, H., 2015. Early Triassic trace fossils from the Three Gorges area of South China: Implications for the recovery of benthic ecosystems following the Permian–Triassic extinction. Palaeogeogr. Palaeoclimatol. Palaeoecol. 429, 100–116.

Zheng, Y. F., Xiao, W. J., Zhao, G. C., 2013. Introduction to tectonics of China. Gondwana Res. 23, 1189–1206.

Zonneveld, J.-P., Gingras, M.K., Beatty, T.W., 2010. Diverse ichnofossil assemblages following the P–T mass extinction, Lower Triassic, Alberta and British Columbia, Canada: evidence for shallow marine refugia on the northwestern coast of Pangaea. Palaios 25, 368–392.

Table 1. Major characteristics of ichnotaxa documented in this study.

Ichnotaxa	Description	Possible trace-maker
Arenicolites isp. (Fig. 6A, F)	Paired burrows on bedding planes with absence of disturbed sediments between tube pairs or dumbbell-shaped structures. Burrows with diameters ranging from 8–15 mm, the distance between two paired burrows is between 30-50 mm. U-shaped burrows in sandstone beds. Poorly preservation identical it to *Arenicolites* isp. (Rindsberg and Kopaska-Merkel, 2005).	Polychaetes, small crustacean
Asteriacites lumbricalis (Fig. 4)	Star-shaped traces, owning central disc-shaped area of pentagonal outline with five lagre length:width ratio arms originating from its corners. The arms documented from the HZGM are 10–20 mm long, 2 mm wide, and the central disc measures ca. 5 mm. The length:width ratio of the arms is 5–10. The newly obtained specimens are assignable to *A. lumbricalis* due to the central disc-shaped area, as well as lagre length:width ratio (Baucon and De Carvalho, 2016; Knaust and Neumann 2016).	Ophiuroids
Biformites zhadaensis (Fig. 5)	Narrow, bedding-parallel, hook-shaped or sinuous imprints. *Biformites* is interpreted to be produced by ophiuroids and asteroids by means of locomotion on the sediment surface. The newly obtained specimens are assignable to *Biformites zhadaensis* due to the delicate, ideally bisymmetrically arranged, transverse (elongate, or polygonal) protuberances of the imprints of arms of walking ophiuroids (Bell, 2004; Schlirf, 2012; Knaust and Neumann, 2016).	Ophiuroids
Dendrotichnium isp. (Fig. 6C–D)	Horizontal, tree-like trails, consists of a central branch and several lateral branches arranged symmetrically on each side of the central main branch. The main branch is larger in size and more direct in shape. The main branch is 10 cm in length, 5mm in diameter, while lateral branches are generally about 2mm in diameter. The features are not obvious, thus the species cannot be identified (Häntzschel, 1975).	Myriapod, or other arthropods
Didymaulichnus lyelli (Fig. 6E)	Horizontal, simple, unbranching smooth bilobate trails with characteristic two convex ridges and a smooth median furrow. Trace preserved as positive relief. Burrows have variable lengths with exposure, with average width ~10 mm (Chen et al., 2011).	Gastropods, arthropods, polychaete-like worms
Dimorphichnus isp. (Figs. 7A–C, F)	Comprises asymmetrical trackways involving two types of imprints: elongated scratches or raker marks and blunt imprints. Imprints vary between 3 to 10 mm long but are relatively uniform in size within the row. Imprint pace is 7 to 11 mm and relatively uniform within one series (Hofmann et al., 2012).	Arthropods
Diplichnites isp. (Figs. 7B, 8C, E–H)	A pair of blunt imprints on bedding planes, parallel to each other. Individual blunt may extended oblique angle with the direction of the whole imprints. The external width of the *Diplichnites* trackway is 30 mm and the minimum internal width about 10 mm (Briggs et al., 2010).	Arthropods
Kouphichnium	Toe-shaped footprints, always consist of several rows, individual pedate	Arthropods

isp. (Fig. 8D)	track contains 2–4 toes, and always sharply tailing-out. A continuous trail occurs occasionally between the set of footprints. *Kouphichnium* has been rarely recorded from the Lower Triassic successions (Häntzschel, 1975).	
Laevicyclus mongraensis (Fig. 6J)	This ichnotaxon is rarely present in the HZGM collection and is preserved as regular concentric circles with a central canal in plane view. This vertical trace is perpendicular to the bedding plane with a circular outline on the upper surface of sandstone beds. The HZGM traces resemble *Laevicyclus mongraensis* in size and morphology (Chen et al., 2012).	Worm, with tentacle swirl-marks
Monomorphichnus isp. (Figs. 7A, C, E, 8F)	A set of hotizontal scratch marks, preserved as convex ridges. The ridge parallel to each other. Each set of ridges contains 5–7 ridges, among which one is wider than others. The ridges of *Monomorphichnus* are equidistant and 15 to 30 mm long. Spacing between ridges is about 2 mm. Ridges are up to 1 mm wide (Hofmann et al., 2012).	Arthropods
Phycodes isp. (Fig. 6B)	Bundle-like burrow, parallel to the bedding plane, The Bundle-like burrow contains a main tube and several lateral tubes, the lateral tubes arranged in both sides of the main tube. The main tube and lateral tubes are almost the same size, ~4 mm. The main tube is straight, while the lateral tube curves. *Phycodes* has been considered as standardized trace fossils of the shallow marine facies. Common in tide flat, prodelta, lagoon and offshore, but even in brackish water environment and deep water (Häntzschel, 1975).	Wormlike animal, pennatula animal and sea pens
Planolites montanus (Fig. 6E–H)	Subcylindrical horizontal burrows with smooth surfaces. Burrow is straight to gently curved, with diameters ranging from 2–14 mm. Burrow fill is a darker color than host rock. Burrows are usually filled with sediment different from host rock. Burrows are typically 2–5 mm in diameter, occasionally intersect each other. *P. montanus* can accommodate these simple, horizontal burrows (Chen et al., 2011).	Polychaetes or worm-like creatures
Planolites isp. (Fig. 6I)	Subcylindrical horizontal burrows with transverse ornamentation. Burrow is straight, typically 4–6 mm in diameter.	Worm-like creatures
Protovirgularia isp. (Fig. 8B)	Keel-like trail, slightly winding, ~8 mm in width, consisting of a median furrow with lateral, generally paired, bilaterally symmetrical, narrow wedge-shaped appendages (Knaust, 2014). Keel-like burrow with triangular cross-section, straight, ca 14 mm wide, bilobated, with successive pads of sediment expressed as chevron-like ribs on the exterior.	Cleft-foot bivalve
Ptychoplasma isp. (Figs. 7C, 8A)	Preserved as positive hyporelief, Straight to slightly winding chain of mostly conical mounds, which can partly overlap (Knaust, 2014). Consists of rather tall hypichnial ridges whose width pinches and swells longitudinally, consisting in some places of a smooth wall-like ridge and in others of a series of relatively deep amygdaloid nodes. Both styles of ridge have an imbricate fill as shown by low-angle ornament on the sides. *Ptychoplasm*a was firstly interpreted as a gastropod trail. The amygdaloid swellings are similar to the bivalve resting trace *Lockeia* (Uchman, et al., 2011).	Wedge-foot bivalves
Treptichnus pedum	The feature that distinguishes *Treptichnus pedum* from ordinary worm burrows is its subdivision into modular segments. They look like buds	Worm-like deposit-feeders

(Figs. 7C, 8A)	along a twig, while the burrow as a whole does never branch, but may follow a straight, sinusoidal, or coiled course. *T. pedum* is usually preserved as positive hyporelief. All features justify the assignment to *T. pedum*. The first appearance of *T. pedum* has been used to indicate thhe Ediacaran-Cambrian boundary (Seilacher, 2007; Buatois et al., 2013).	
Undichna isp. (Figs. 7D)	The fish swimming trace *Undichna* contains a set of sinusoidal drag marks with a common wave length and alignment. Individual drag marks may be continuous, or the troughs/crests may be preferentially absent or preferentially present. There may be up to five sinusoidal elements in a set. Waves occur as non−parallel pairs which are intertwined. The traces are preserved as impressions on bedding surfaces of siltstone (Wisshak et al., 2004). The wave-shaped trace is 25 mm wide and extends over 15 cm across the slab. The wavelength of all waves is ~40 mm, and their amplitudes decrease outward from 20 mm to 12 mm. Both the wavelength and amplitude are constant (Lu et al., 2012).	Fish swimming trace

Fig. 1. A, Geographic map of Shaanxi Province, western North China showing location of the Houzhougongmiao (HZGM) section, Linyou county. **B**, Early Triassic paleogeographic map of the South China block (base map follows Liu et al., 2015) showing the position of the studied section (red square).

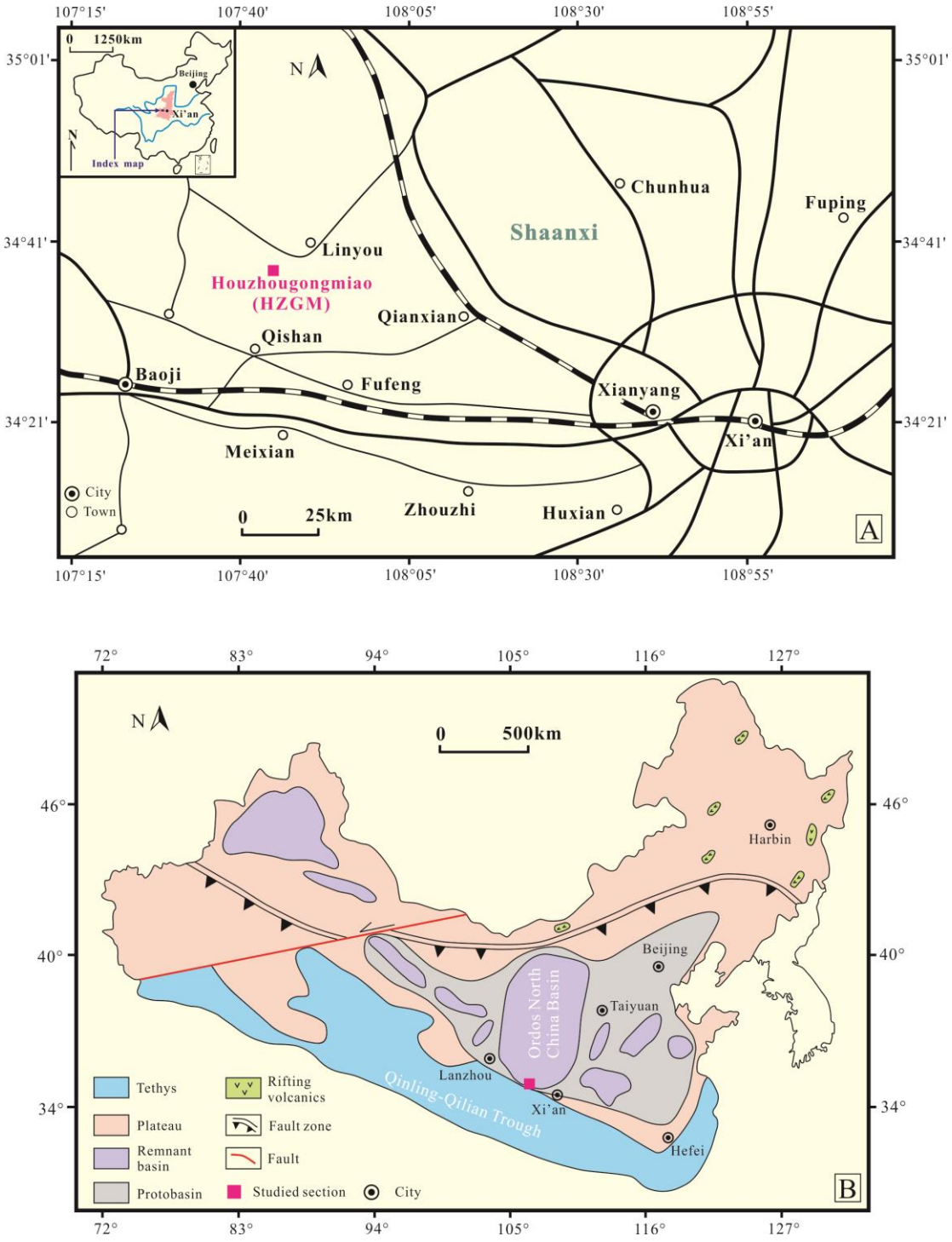

Fig. 2. A, Columnar section of the Lower Triassic succession exposed at the HZGM section. **B**, Logged section showing detailed lithologies of the upper Sunjiagou Formation (Induan) and stratigraphic distributions of ichnotaxa. Bedding plane bioturbation indices (BPBI) are evaluated based on the degree of bedding plane coverage by burrows (Miller and Smail, 1997), which range from 1 to 5, indicating coverage from least to most, respectively.

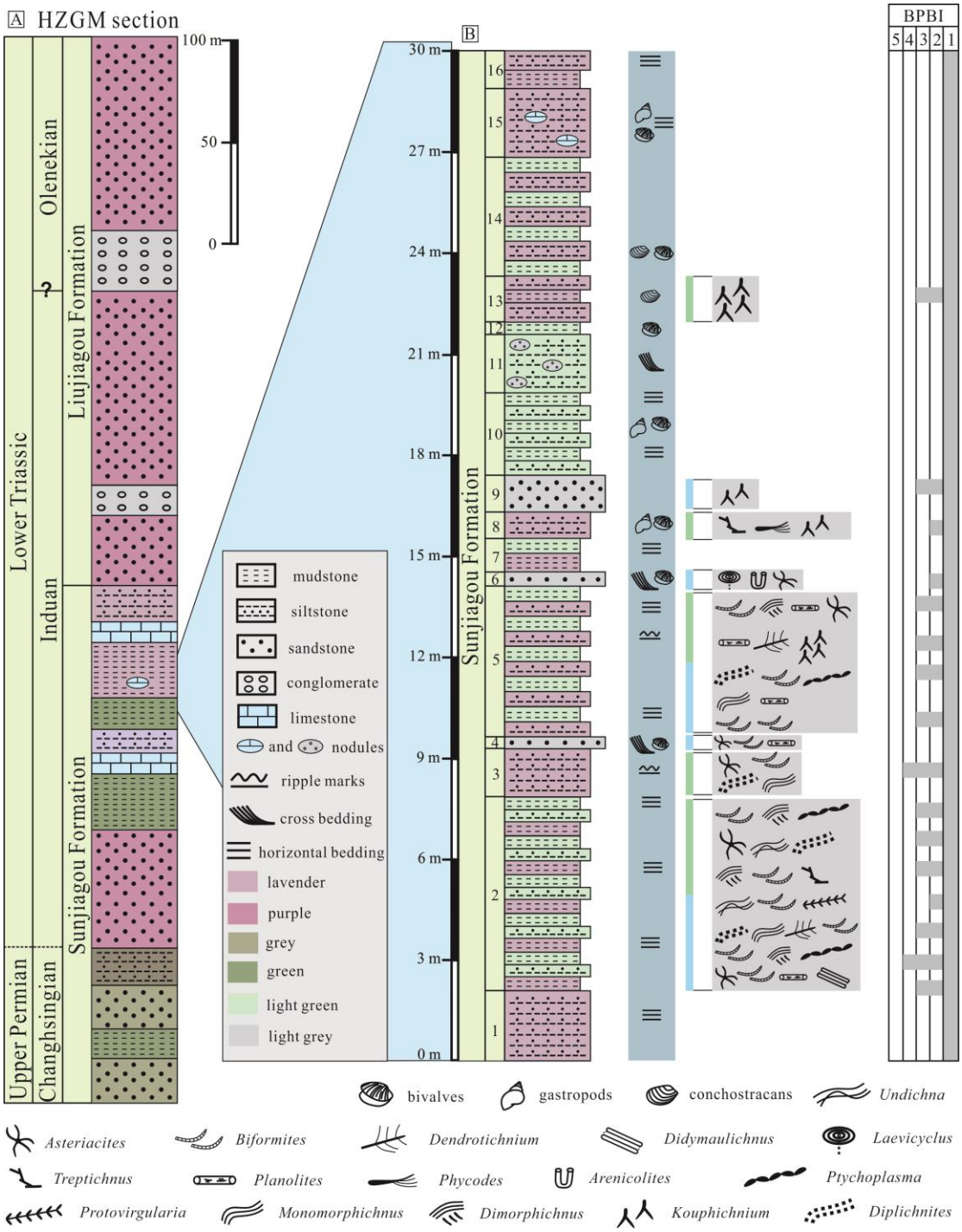

Fig. 3. Field photos of the Lower Triassic succession from the HZGM section. **A**, Medium- to thick-bedded sandstone interbedded with thin-bedded siltstone from the lower Sunjiagou Formation. **B–D**, Thin-bedded siltstone, mudstone beds, together with few sandstone beds (white dotted line in B) make up the studied Induan succession of the upper Sunjiagou Formation. Horizontal beddings are common in siltstone and mudstone beds. **E**, Faint ripple marks from siltstone beds of the Induan succession. **F**, Cross-beddings from sandstone beds of the Induan succession. **G**, Abundant *Biformites* imprints produced by ophiuroids from siltstone beds of the Induan succession. **H**, Conchostracans from mudstone of the upper Sunjiagou Formation. **I**, bivalve fossil *Eumorphotis* sp., from siltstone beds of the upper Sunjiagou Formation.

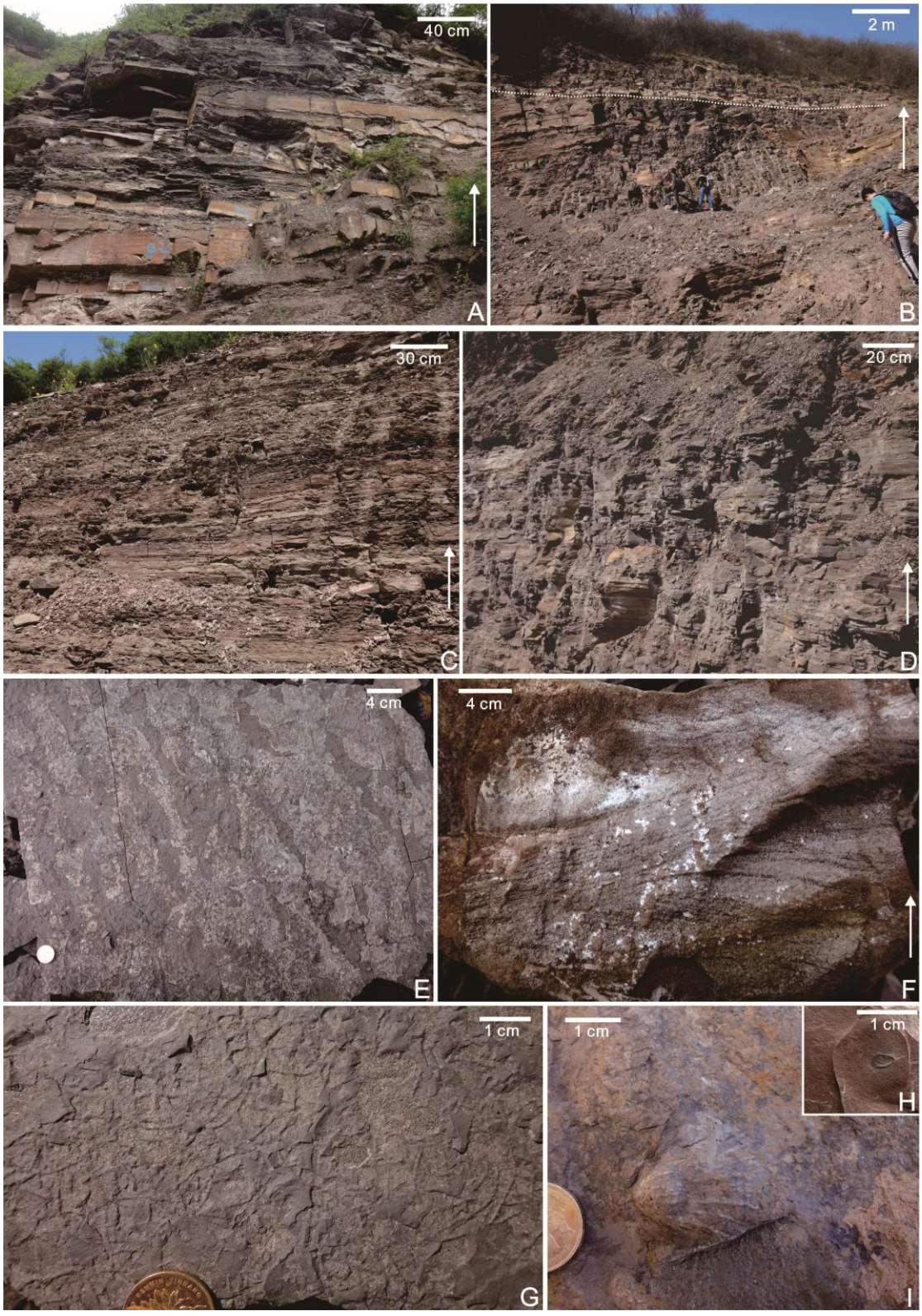
40 cm
A
2 m
B
30 cm
C
20 cm
D
4 cm
E
4 cm
F
1 cm
G
1 cm
1 cm
H
I

Fig. 4. *Asteriacites lumbricalis* from thin-bedded siltstone and sandstone beds; most specimens are preserved as convex hyporelief. A central disc is visible from B, D and I. Hook-shaped imprints of *Biformites* are visible from A and G (white arrows).

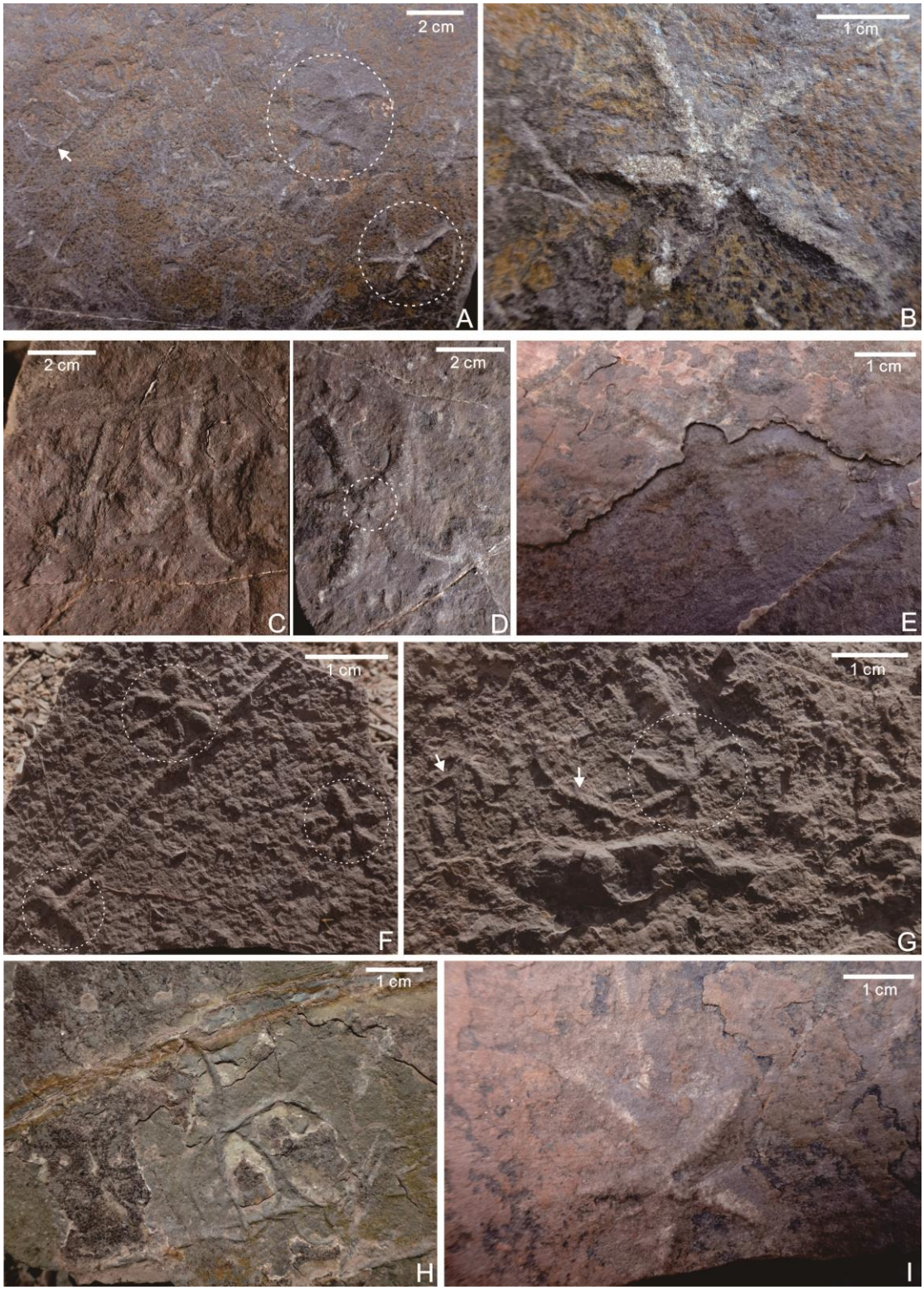

Fig. 5. *Biformites zhadaensis* from thin-bedded siltstone and mudstone beds. Most specimens are preserved as convex epirelief, except for G which is concave epirelief. B, E, and G are composed of a cluster of arcuate or hook-shaped imprints. All specimens possess slightly tapering terminations. Bisymmetrically arranged, transverse protuberances are visible from A, C, E–F, which are identical to the casts of ophiuroid arms.

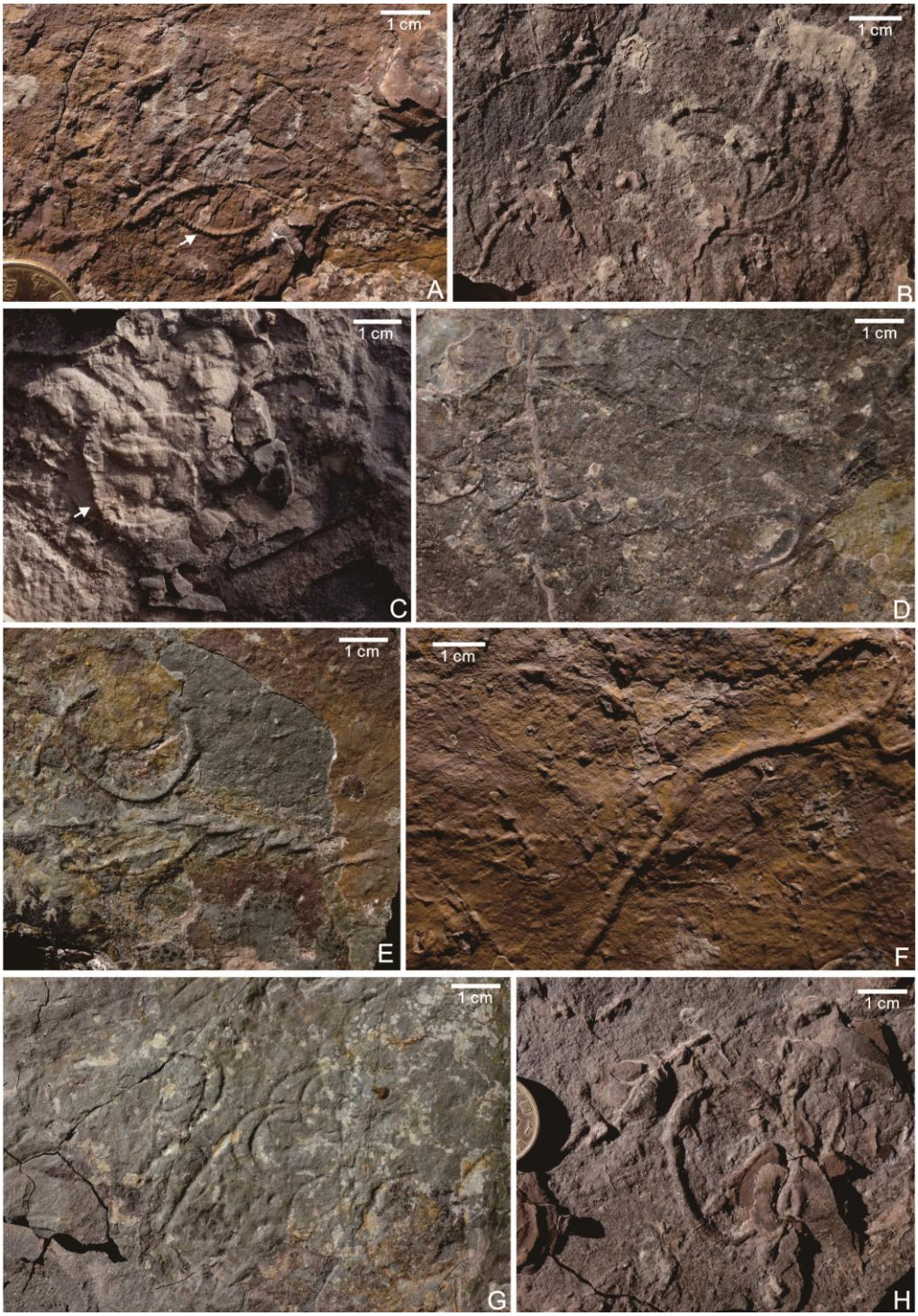

Fig. 6. Burrow-form traces from the upper Sunjiagou Formation in the HZGM section. **A**, **F**, *Arenicolites* isp. from the upper surface of sandstone bed. **B**, *Phycodes* isp. from the upper surface of Bed 8. **C–D**, *Dendrotichnium* isp. from the upper surface of Bed 5. **E**, *Didymaulichnus lyelli* from the upper surface of Bed 2. **G–H**, Small *Planolites montanus* from the upper surface of siltstone beds. **I**, *Planolites* isp. from the upper surface of mudstone of Bed 5. Abundant longitudinal ornaments are visible. **J**, *Laevicyclus mongraensis* from the upper surface of sandstone of Bed 6.

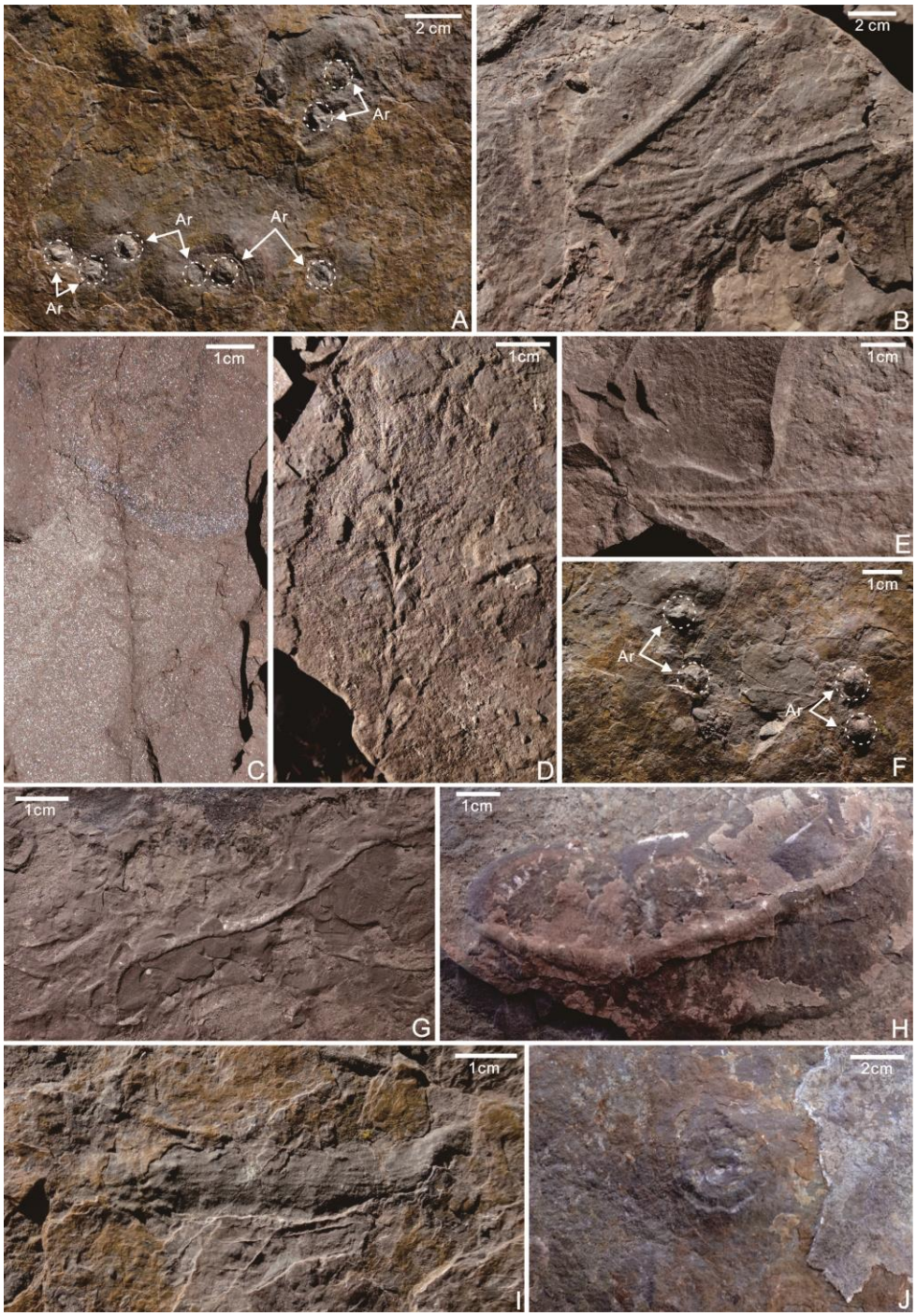

Fig. 7. Arthropod trackways and fish swimming traces on the upper surface of siltstone beds. **A**, *Dimorphichnus* isp. (Dim, blue dotted block) and *Monomorphichnus* isp. (Mop, white dotted block), from the upper surface of siltstone of Bed 2. Blunt imprints (blue arrow) are preserved together with the elongated scratches. **B**, *Dimorphichnus* isp. (Dim, blue dotted block) and *Diplichnites* isp. (Dip) from the upper surface of siltstone of Bed 5. Blunt imprints (blue arrows) are visible. **C**, *Dimorphichnus* isp. (Dim, blue dotted block), *Monomorphichnus* isp. (Mop), *Ptychoplasma* isp. (Pty), and *Treptichnus pedum* (Tre), are preserved together on the upper surface of siltstone of Bed 5. **D**, *Undichna* isp., fish swimming trace preserved as convex hyporelief of Bed 2. **E**, *Monomorphichnus* isp. (Mop), from the siltstone bed. **F**, *Dimorphichnus* isp., (Dim, white arrow) from the upper surface of siltstone of Bed 5. Blunt imprints (blue arrows) are visible.

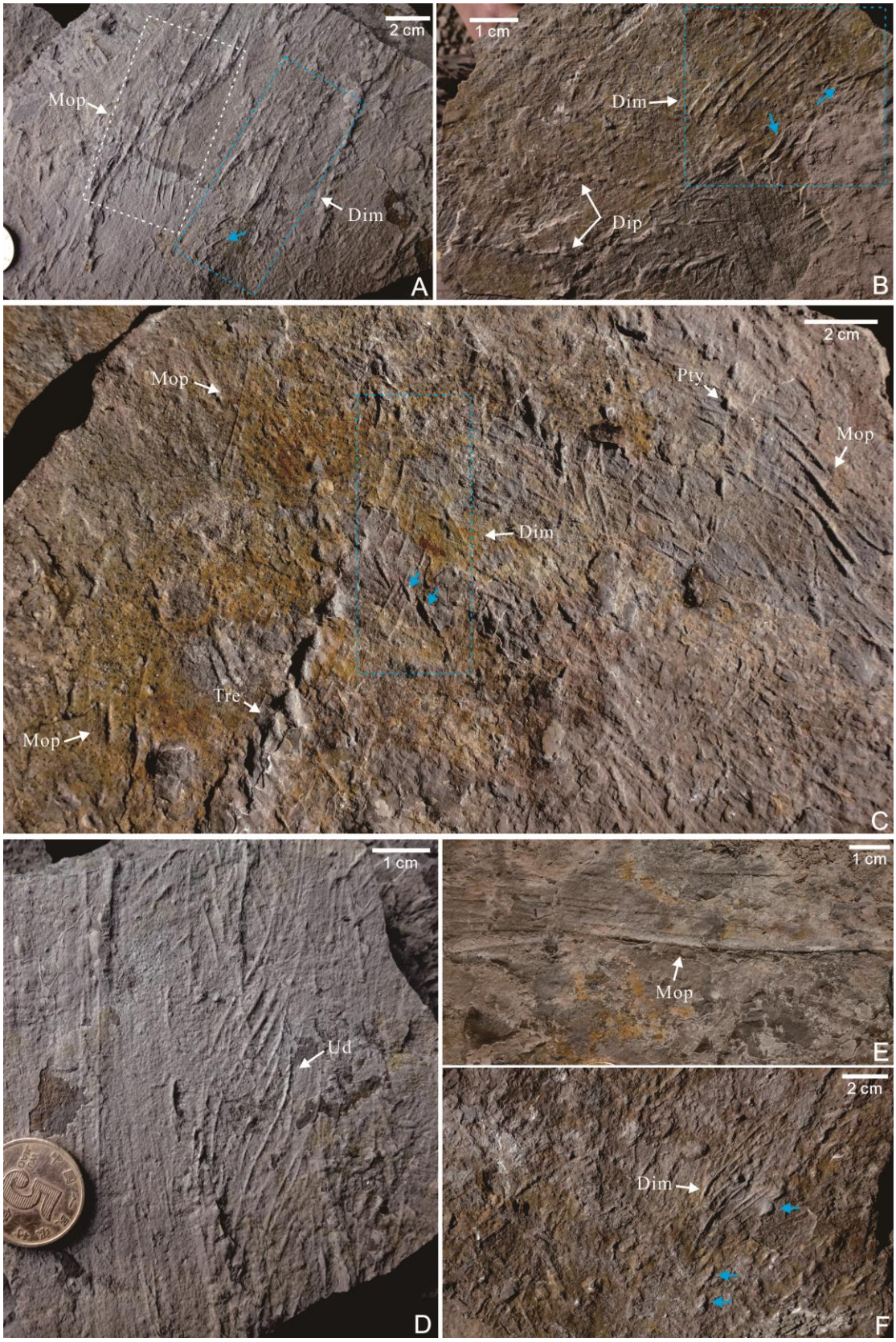
2 cm
Mop
Dim
A
1 cm
Dim
Dip
B
2 cm
Mop
Pty
Mop
Dim
Tre
Mop
C
1 cm
Ud
D
1 cm
Mop
E
2 cm
Dim
F

Fig. 8. Arthropod trackways and other traces. **A**, *Ptychoplasma* isp. (Pty), and *Treptichnus pedum* (Tre), from the upper surface of siltstone of Bed 2. **B**, *Protovirgularia* isp. (Pro), from the mudstone bedding plane of Bed 2. **C**, *Diplichnites* isp. (Dip) from the upper surface of siltstone of Bed 2. **D**, *Kouphichnium* isp. (Kou), from siltstone beds. **E**, *Diplichnites* isp. (Dip) from the upper surface of siltstone of Bed 5. **F**, *Monomorphichnus* isp. (Mop), and *Diplichnites* isp. (Dip) preserved together on the upper surface of siltstone of Bed 5. **G–H**, *Diplichnites* isp. (Dip, dotted lines) from the upper surface of siltstone of Bed 2.

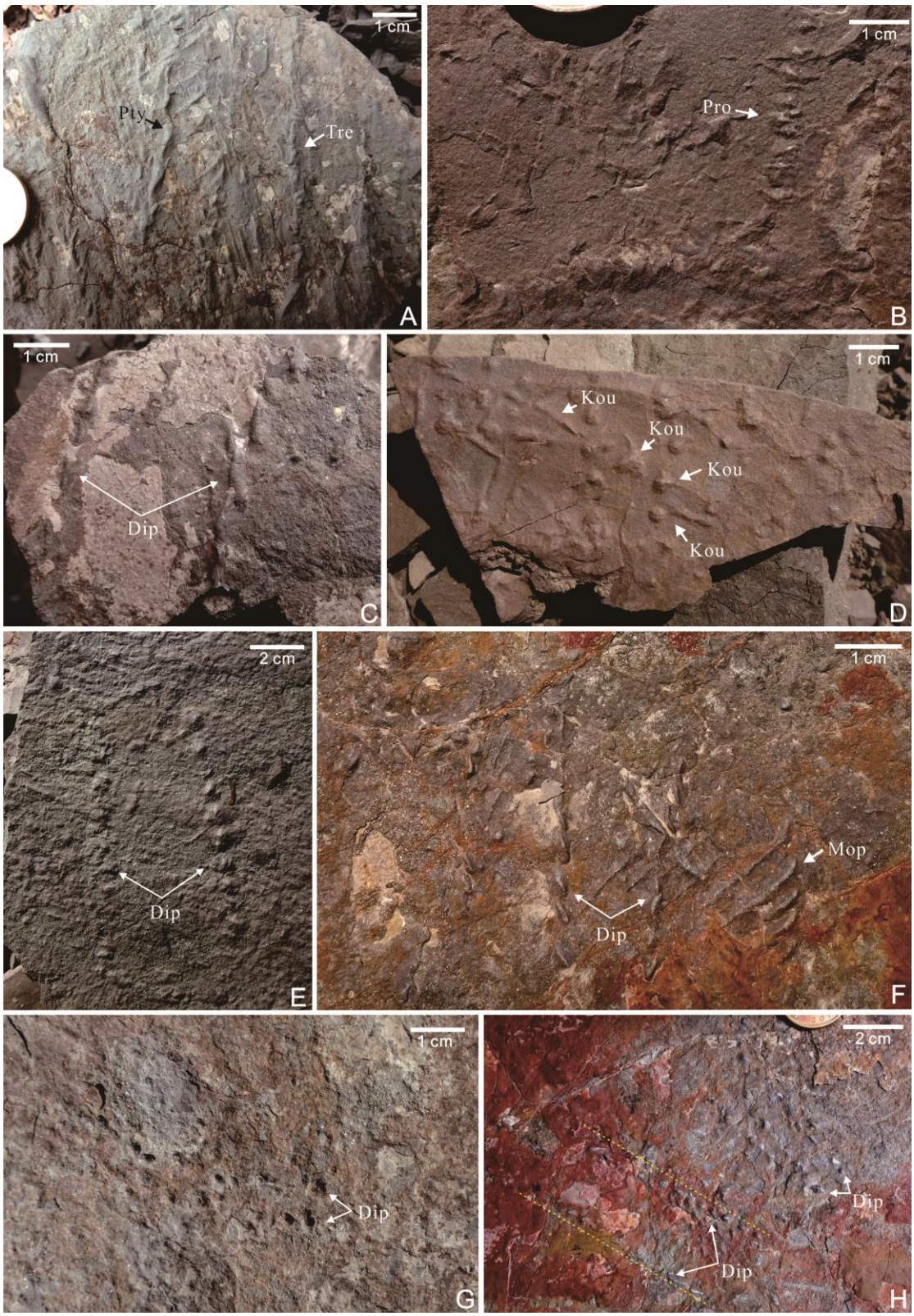
1 cm
Pty
Tre
A
1 cm
Pro
B
1 cm
Dip
C
1 cm
Kou
Kou
Kou
Kou
D
2 cm
Dip
E
1 cm
Mop
Dip
F
1 cm
Dip
G
2 cm
Dip
Dip
H

Fig. 9. A, Pie diagram of the upper Sunjiagou Formation ichnoassemblage from the HZGM section showing the percentage of trace types based on the number of ichnotaxa. **B**, Pie diagram showing the ichnofaunal percentage of each trace type based on trace abundance.

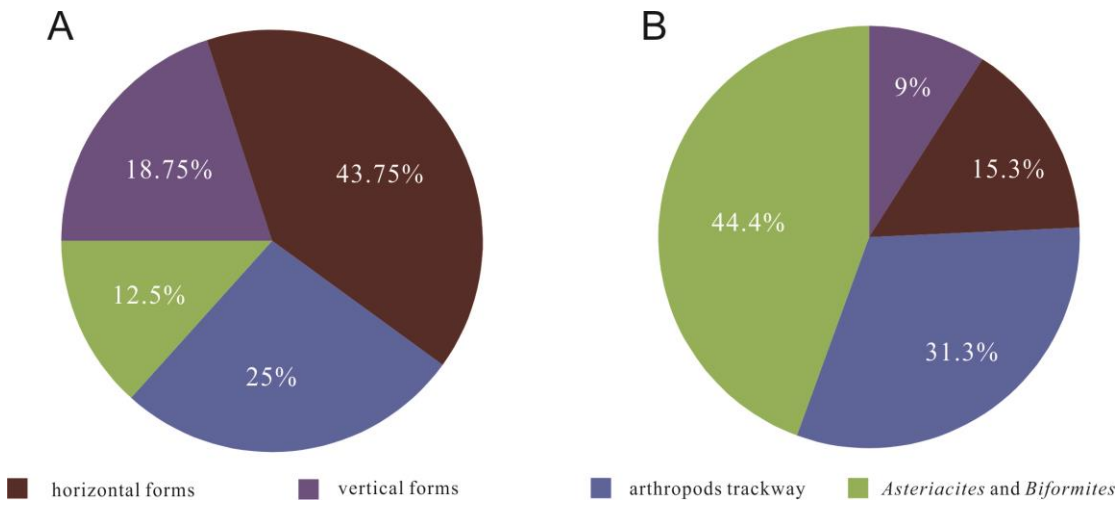

Fig. 10. A, Plot diagram of arm length vs arm width of *Asteriacites lumbricalis* from the HZGM section. **B**, Distribution of the size of central disc of the *Asteriacites lumbricalis*. **C**, Distribution of the burrow size of *Biformites zhadaensis*.

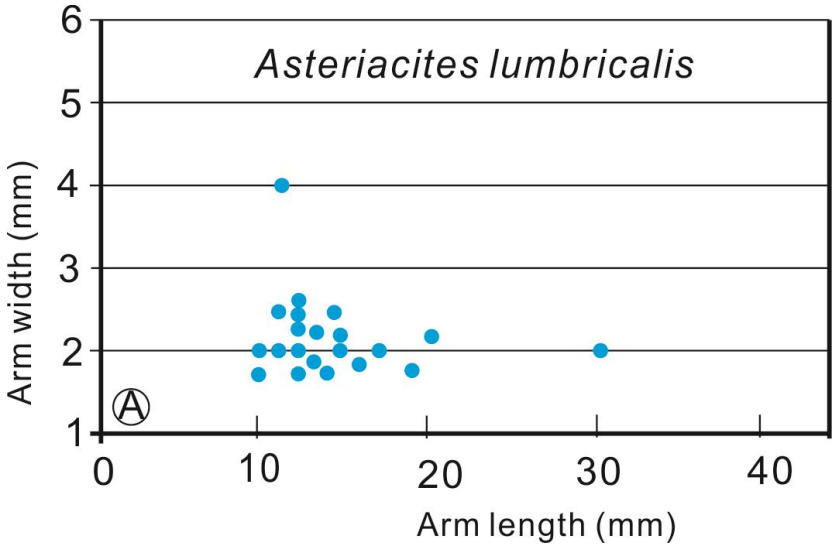
Asteriacites lumbricalis
Arm width (mm)
Arm length (mm)
Ⓐ
1
2
3
4
5
6
0
10
20
30
40

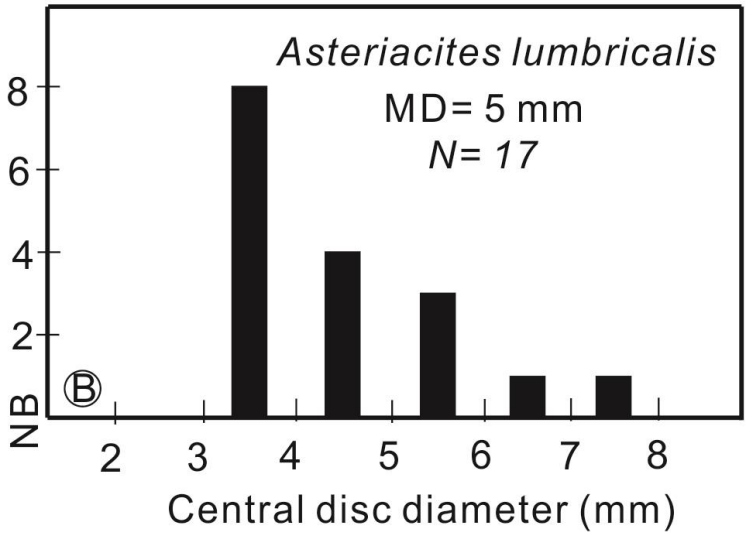
Asteriacites lumbricalis
MD= 5 mm
N= 17
NB
Central disc diameter (mm)
Ⓑ
2
4
6
8
2
3
4
5
6
7
8

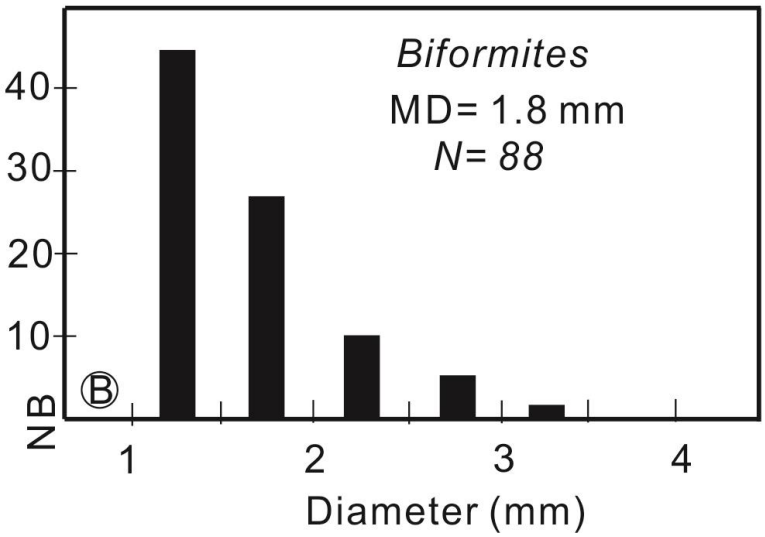
Biformites
MD= 1.8 mm
N= 88
NB
Diameter (mm)
Ⓑ
10
20
30
40
1
2
3
4

Fig. 11. Sketch map showing various behaviors of ophiuroids to produce different ichnofossils. **A**, Resting trace *Asteriacites lumbricalis*. **B**, Imprints of arms of walking ophiuroids.

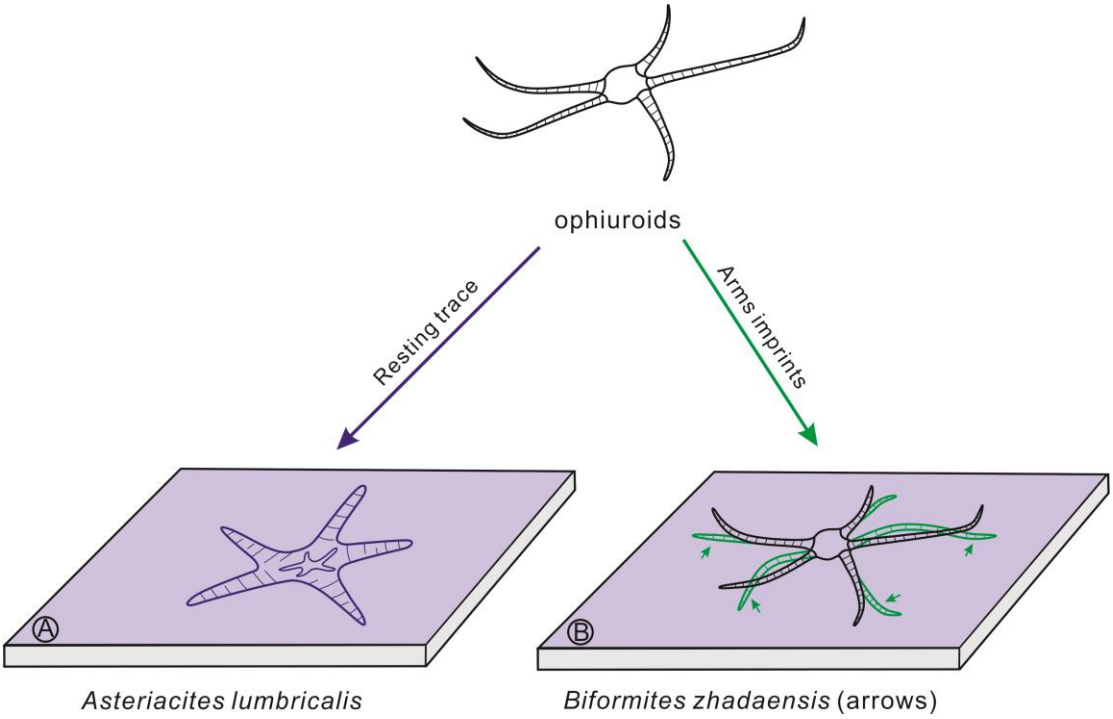

Fig. 12. Global distributions of ichnodiversity both in the Induan and Olenekian (base map follow Scotese, 2014). Ichnodiversity is represented by the number of ichnotaxa. Low ichnodiversity = 0–2 ichnotaxa; moderate ichnodiversity = 3–10 ichnotaxa; high ichnodiversity = >10 ichnotaxa (Ichnodiversity classification is based on Beatty et al., 2008). 1, HZGM section, North China (this study). 2, Western Spitsbergen (Wignall, 1998); 3, British Columbia, Western Canada (Beatty et al., 2008; Zonneveld et al., 2010); 4, Persian Gulf, Iran (Knaust, 2010); 5, Northern Italy (Hofmann et al., 2011); 6, Northern Italy (Twitchett and Wignall, 1996; Twitchett, 1999); 7, Carnic Alps, Italy (Baucon and De Carvalho, 2016); 8, Northern Hungary (Foster et al., 2015); 9, Utah, USA (Fraiser and Bottjer, 2009; Hofmann et al., 2015); 10, Western USA (Pruss and

Bottjer, 2004); 11, Western USA (Mata and Bottjer, 2011); 12, Wyoming, USA (Lovelace and Lovelace, 2012); 13, Spitsbergen, Svalbard (Uchman et al., 2016); 14, Lower Yangtze region, South China (Chen et al., 2011; Luo et al., 2016); 15, Middle Yangtze region, South China (Zhao et al., 2015; Feng et al., 2017); 16, Upper Yangtze region, South China (Shi et al., 2015; Luo et al., 2016). 17, Western Australia (Chen et al., 2012); 18, Karoo Basin, South Africa (Bordy and Krummeck, 2016); 19, Henan Province, North China (Hu et al., 2009, 2015).

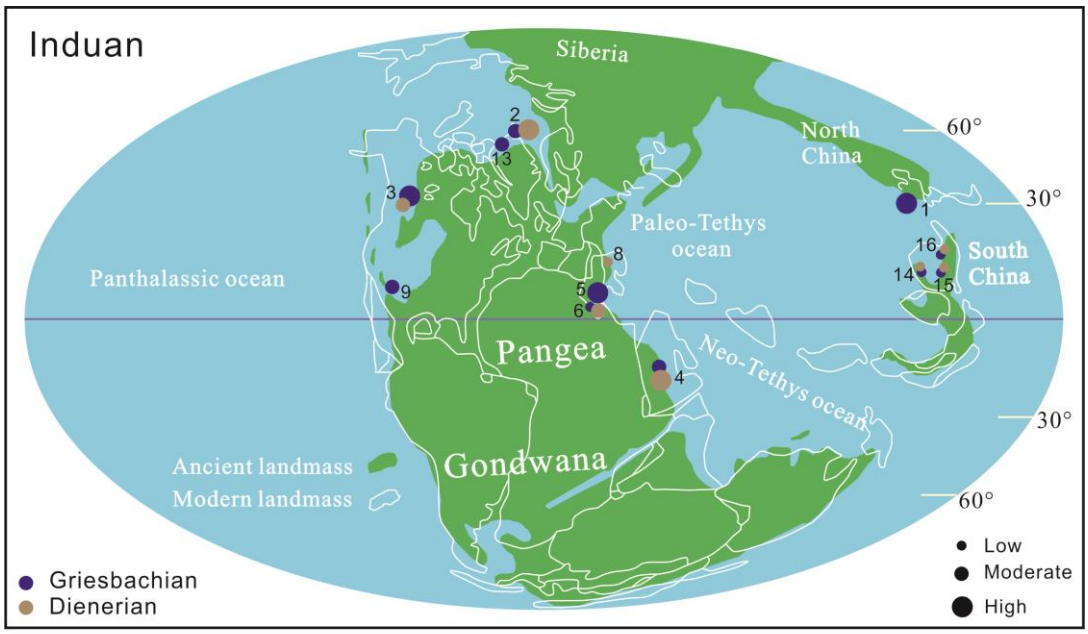

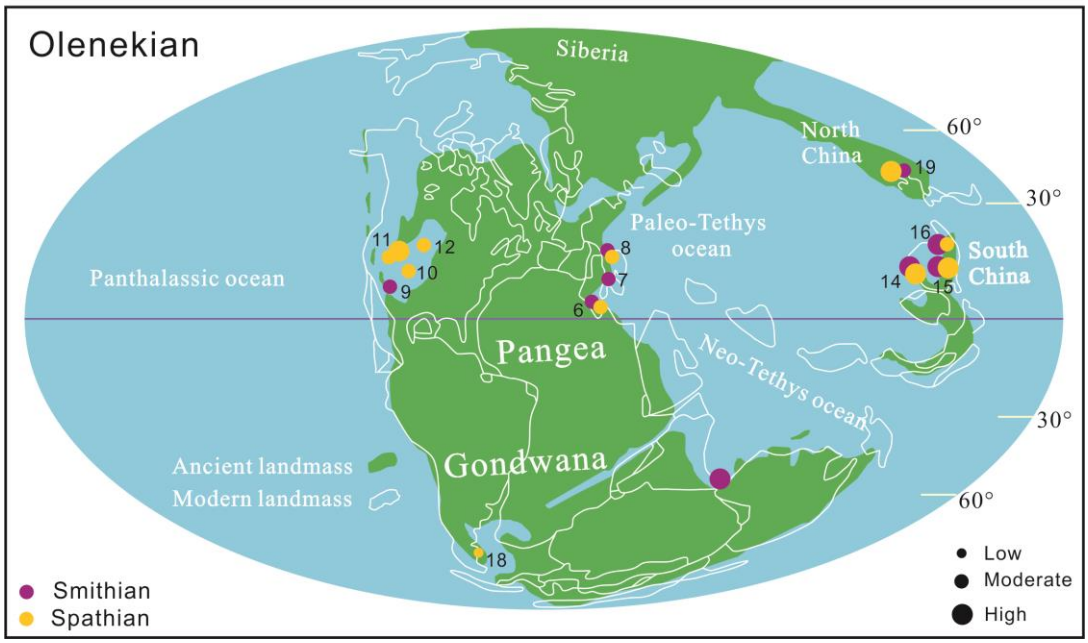

Fig. 13. Sketch reconstructions showing three different types of ichnoassemblages lived in the Induan. **A**, Only simple, horizontal *Planolites* burrows. **B**, The studied HZGM ichnoassemblage, diverse ichnotaxa, but composed mainly of shallow tiers and scratches marks or trackways produced by arthropods. **C**, diverse ichnotaxa, characterized by complex burrow forms, such as *Thalassinoides*, *Rhizocorallium* and *Diplocraterion*. This type has been reported from four localities from both high- and low-latitudes all around the world.

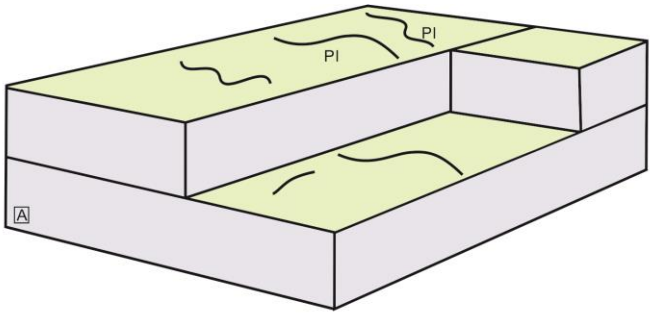

Pl: *Planolites*

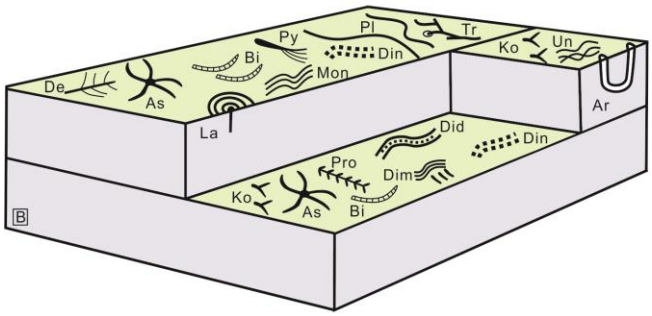

Ar: *Arenicolites* As: *Asteriacites* Did: *Didymaulichnus* Dim: *Dimorphichnus* Din: *Diplichnites*
Bi: *Biformites* De: *Dendrotichnium* La: *Laevicyclus* Mon: *Monomorphichnus* Pl: *Planolites*
Py: *Phycodes* Pro: *Protovirgularia* Ko: *Kouphyichnium* Tr: *Treptichnus* Un: *Undichna*

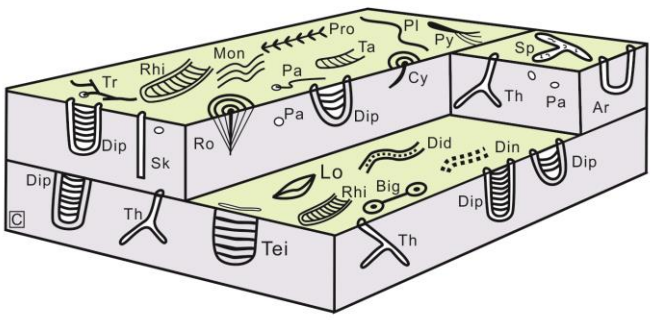

Ar: *Arenicolites* Did: *Didymaulichnus* Dip: *Diplocraterion* Lo: *Lockeia* Mon: *Monomorphichnus*
Pa: *Palaeophycus* Pl: *Planolites* Py: *Phycodes* Sk: *Skolithos* Ro: *Rosselia* Rhi: *Rhizocorallium*
Ta: *Taenidium* Th: *Thalassinoides* Tei: *Teichichnus* Big: *Bifungites* Pro: *Protovirgularia*
Cy: *Cylindrichnus* Din: *Diplichnites* Tr: *Treptichnus*